LA-3880-MS

LOS ALAMOS SCIENTIFIC LABORATORY
of the
University of California
LOS ALAMOS • NEW MEXICO

Quarterly Status Report on the Advanced Plutonium Fuels Program October 1-December 31, 1967

UNITED STATES
ATOMIC ENERGY COMMISSION
CONTRACT W-7405-ENG. 36

DISCLAIMER

This LA...MS report presents the status of the LASL Advanced Plutonium Fuels Program. Previous Quarterly Status Reports in this series, all unclassified, are:

LA-3607-MS
LA-3650-MS
LA-3686-MS
LA-3708-MS*
LA-3745-MS
LA-3760-MS*
LA-3820-MS

This report, like other special-purpose documents in the LA...MS series, has not been reviewed or verified for accuracy in the interest of prompt distribution.

*Advanced Reactor Technology (ART) Series

LA-3880-MS
SPECIAL DISTRIBUTION

LOS ALAMOS SCIENTIFIC LABORATORY
of the
University of California
LOS ALAMOS • NEW MEXICO

Report distributed: February 20, 1968

Quarterly Status Report on the Advanced Plutonium Fuels Program October 1-December 31, 1967

FOREWORD

This is the sixth quarterly report on the Advanced Plutonium Fuels Program conducted at the Los Alamos Scientific Laboratory. A comparison of this issue with the previous quarterly report will show that accounts of additional areas of study have been included in the current document. These investigations, described in this report under the heading "Other Advanced Systems," were formerly reported in LAMS documents titled "Advanced Reactor Technology," a series which has now been discontinued.

Starting in January 1968, the LASL Advanced Plutonium Fuels Program was expanded to include work on solid metallic fuel systems for fast reactor (Project 824). Reporting of this work will begin in the next issue of this series.

Most of the investigations discussed here are of the continuing type. The results and conclusions described may therefore be superseded as the program progresses. Published reference to these preliminary results, or quotations of them, should not be made without obtaining explicit permission to do so from the person in charge of the work.

TABLE OF CONTENTS

TABLE OF CONTENTS
(continued)

PROJECT 801

SODIUM TECHNOLOGY

Person in Charge: D. B. Hall
Principal Investigators: G. H. Best
R. H. Perkins

I. INTRODUCTION

High-temperature sodium systems, such as those contemplated for use in fast, central-station-reactor concepts, require a high level of purity control to limit corrosive processes and to preserve reliability. In addition, the advent of large sodium-cooled fast reactors requires a knowledge of fission product release and distribution in the primary coolant system and the development of methods by which this distribution can be altered. To monitor the impurity levels in coolant sodium (and in its associated cover gas system), suitable instrumentation and analytical techniques must be developed. Methods and kinetics of impurity control are studied using these analytical devices as they become available.

The release and distribution of fuel and fission products in sodium systems have been studied using both sealed capsules and forced-convection sodium loops. Preliminary experiments have been performed on the release of fission products from trace-irradiated (U,Pu)C fuel into a sodium column under isothermal conditions and with an axial temperature gradient. Similar experiments have been initiated to study the distribution of individual long-lived gamma-active isotopes in a sealed capsule containing sodium and a potential trapping material.

Long-lived fission products have been introduced into a small, forced-convection sodium loop by immersing a trace-irradiated plutonium alloy in the flowing sodium. The distribution of plutonium, ^{90}Sr, ^{137}Cs, and ^{155}Eu in the loop, over periods of 1000-3000 h, has been observed by *in situ* gamma scanning of loop components and by radiochemical analysis of traps and metal specimens removed from the loop. Hot trapping, cold trapping, and graphite adsorber experiments have been conducted.

The solubility of oxygen in sodium using the vacuum-distillation analytical technique has been determined over the temperature range of 125° to 300°C. An experimental facility to be used for the development of analytical techniques for the measurement of impurities in sodium has been constructed and is being tested. Another sodium loop which will be used in the development of in-line instrumentation and investigation of the soluble gettering technique for impurity control is being built.

The performance characteristics of different designs of cold traps for sodium systems are being determined. Several tests were conducted to determine the rates of change of oxygen concentration in a system following rapid changes in the cold trap temperature. Methods to measure the rate at which gases diffuse into sodium loops have now been tested. Results are encouraging. The fabrication of artificial leaks in sodium containers is continuing. If the program is successful, it may be possible to establish pre-operational testing standards which will insure satisfactory service life for sodium loop components.

II. TRANSPORT AND DISTRIBUTION OF FISSION PRODUCTS IN SODIUM: LOOP EXPERIMENTS
(J. C. Clifford)

A. General

The behavior of radioactivity released to

sodium from failed or vented fuel elements may limit access to portions of the primary coolant system and may affect the consequences of a loss-of-coolant incident. Depending on the fission-product release fraction anticipated in either circumstance, it may be desirable to scavenge these species (as well as uranium and plutonium) from the coolant.

The immediate goals of this investigation are: (1) to identify sodium-soluble fission-product species and (2) to examine the effects of primary-coolant-system construction materials, design features, and operating conditions on these species.

B. Current Results

A forced-convection sodium system has been assembled for studying the release and distribution of ^{131}I, ^{140}Ba, ^{137}Cs and other, less soluble (in sodium) species from trace-irradiated plutonium fuels. The sodium system, which is shown in Fig. 1, consists of a primary loop containing the irradiated

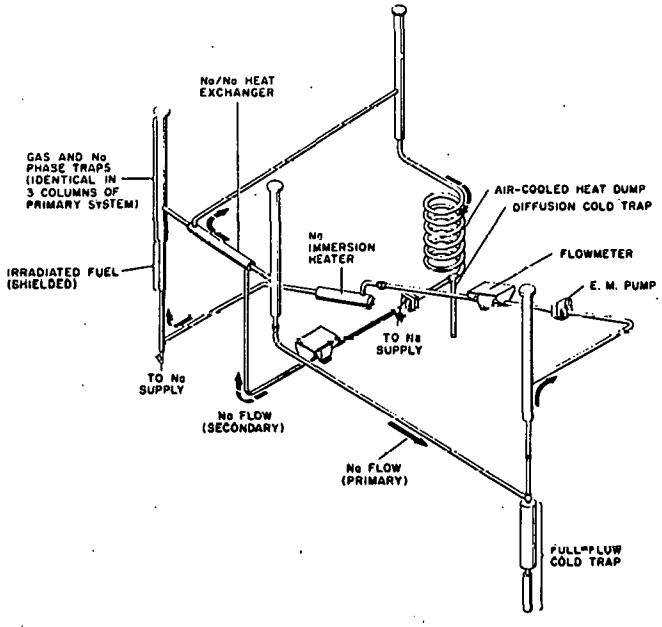

Fig. 1. Sodium system for studying the behavior of fission product Ba, I, and Cs released from irradiated plutonium fuels.

fuel and a secondary, nonradioactive loop for extraction of heat from the primary loop. The primary loop is composed of three similar vertical columns, a heater, heat exchanger, pump, flowmeter, and full-flow cold trap. The vertical columns, the heat exchanger, the full-flow cold trap and their connecting piping lie in the same vertical plane and can be scanned in the vertical and horizontal directions using a high-resolution gamma detector and scanner described previously.[1] The cold trap is connected to the rest of the primary loop with metal-gasketed tube joints and can be replaced with other items as the need arises. The secondary loop consists of the annulus of the Na/Na heat exchanger, an air heat dump, diffusion cold trap, pump, and flowmeter.

The loops are small, containing a total of 3 lb of sodium. The maximum mass flow in each loop is 300 lb/h, and corresponding sodium velocities are approximately 1-1/2 ft/sec in the connecting tubing and 0.1 ft/sec in the vertical columns. The range of operating temperatures is 110°-650°C. At present the primary loop is being hot trapped at 600°C to remove the oxide film from the sodium-wetted stainless steel surfaces.

III. TRANSPORT AND DISTRIBUTION OF FISSION PRODUCTS IN SODIUM: CAPSULE EXPERIMENTS
(J. C. Biery, C. R. Cushing)

A. General

The rupture of nuclear reactor fuel elements containing ceramic Pu-U pellets will allow fission products to be leached from the pellets by the sodium coolant. The release rates of these fission products should be known to evaluate sodium system contamination problems. This research program is designed to determine fission product mass transfer rates from ceramic fuel pellets to sodium as a function of temperature, sodium conditions, and pellet composition.

The release of fission products into sodium from irradiated Pu-U ceramic fuel pellets is being studied by measuring gamma count rate spectra from the pellet and the sodium into which fission products have transferred. The neutron irradiated pellet is enclosed with 3 to 10 in. of sodium in a 12-in.-long capsule. The distribution of fission products as a function of time and position in the capsule is determined by gamma scanning the capsule. The temperatures for the experiments range from 650° to 900°C. The furnace can impose either isothermal conditions or longitudinal temperature gradients up to 25°C/in.

B. Current Results

An experiment designed to study fission product mass transfer from an irradiated (U,Pu)C pellet into sodium was started on December 1, 1967. A 0.244-in.-long x 0.260-in.-diam pellet was irradiated in the Omega West Reactor (OWR) for two periods of 116 h each in an average thermal flux of 8.3×10^{10} n/(cm^2-sec). The number of fissions was 6.7×10^{16} and the number of ^{137}Cs atoms produced was 3.5×10^{15}. The pellet was placed in contact with a 7-in. column of sodium in a 0.430-in.-diam stainless steel tube. The temperature at the pellet was 800°C and at the top of the sodium column it was 700°C.

Counts of the pellet and of the sodium 3 in. above the pellet were made 10 and 11 days after startup. The slit size on the scanner was 1/2 in. high by 3/4 in. wide. The count of the pellet indicated that the detection efficiency of the solid-state detector at a distance of 19 in. from the source varied from 4.5×10^{-5}% to 6.2×10^{-6}%. The sodium count detected measurable amounts of ^{131}I, ^{137}Cs, ^{140}Ba-^{140}La, and ^{144}Ce.

The experiment is utilizing the new solid-state detector-scanner system. The results thus far indicate that the system with the 4096-channel analyzer can detect extremely low concentrations of the fission products in sodium *in situ* as the mass transfer process is occurring. For instance, the concentration of ^{140}Ba-^{140}La, as indicated by the counting rate, is less than 10^{-6} ppm.

IV. TRANSPORT AND DISTRIBUTION OF FISSION PRODUCTS IN SODIUM: CAPSULE EXPERIMENTS WITH SINGLE ISOTOPES

(L. A. Geoffrion, J. M. Williams)

A. General

Capsule experiments have been designed to determine the distribution of gamma-active isotopes in the sodium/stainless steel/helium/adsorber system as a function of time and temperature. The use of gamma-ray scanning will enable the study of transport rates, adsorption and desorption phenomena, and the equilibrium distribution between phases. The isotope ^{137}Cs is the first radioisotope to be studied in these experiments because it is a major fission product released from irradiated nuclear fuels and its 27.7-yr half-life is relatively long. Other candidates for study, using these experimental techniques, are ^{131}I and ^{140}Ba-^{140}La.

The spatial distribution of energetic gamma emitters in small capsules is measured as a function of time and temperature distribution. These measurements are accomplished by gamma scanning the capsule both axially and diametrically while it is moved linearly in 1-mil increments in front of a sodium-iodide detector system. Observations of the approach to equilibrium as a plane ^{137}Cs source diffuses into a cylindrical column of sodium should permit estimations of transport and adsorption rates, distribution coefficients, and diffusion coefficients. Since this method of measurement allows a total mass balance over the system, it should be possible to determine these parameters quantitatively.

B. Current Results

A 12-in.-long, 1-in.-diam stainless steel capsule containing ^{137}Cs on a stainless steel planchet and 6 in. of sodium is now in test. A room temperature axial scan of the capsule after loading showed that most of the cesium was on the planchet. The capsule was then heated isothermally to 200°C and scanned axially and radially. Axial scans at 5, 48, 148, 240, and 312 h indicate that the cesium from the planchet distributes quite slowly. This is in contrast to the rapid cesium redistribution at higher temperatures.

Radial scans taken at 72 and 144 h show a uniform radial concentration of cesium in sodium with little or none on the walls. Previous observations on an 8-in. capsule disclosed significant deposition of cesium on the stainless steel walls in the sodium region when the capsule temperature was lowered to room temperature after holding at 200°C for 200 h.

V. TRANSPORT OF STRUCTURAL, CONTAINER, AND GETTER MATERIALS IN SODIUM

(J. C. Biery, C. R. Cushing)

A. General

Fission product gettering studies have indicated that the use of carbon beds in a sodium system may be useful for ^{137}Cs removal. Carbon, however, is slightly soluble in sodium and can carburize austenitic stainless steels and refractory metals. The temperature dependence of this rate process is not known. Therefore, the purpose of this study is to determine the temperature range in which the

carbon mass transfer rates are sufficiently low to allow use of carbon beds in a sodium system.

The carbon transfer rates from carbon rods will be studied in thermal convection loops. The Type 304 or 316 stainless steel loop itself will serve as the carbon sink when these materials are studied. In a second series of runs, vanadium alloy sleeves will serve as the getters.

B. Current Results

The design of a series of sodium thermal convection loops has been initiated as the first part of the carbon mass transfer program. The loops are to be fabricated from 1-in.-o.d. Type 304 stainless steel tubing, will be 2 ft high and will have cross flow legs 1-1/2 ft long. The loops are designed to control oxygen with diffusion cold traps or by preconditioning with a well-characterized sodium supply. In the latter instance, sodium from the supply system will be pumped through the thermal convection loop for a number of days at the approximate conditions of the subsequent experiment to equilibrate the stainless steel surfaces with the desired oxygen concentration in the sodium. The hot zone of the loops will operate in the 300°-600°C range, and the flow rates during thermal convection operation are estimated to be in the 3-4 cm/sec range.

VI. SAMPLING AND ANALYTICAL TECHNIQUES
(V. J. Rutkauskas, G. E. Meadows, K. S. Bergstresser)

A. General

Dynamic in-line sodium sampling techniques for the vacuum distillation analytical method are presently being evaluated. The objective of this phase of the program is to develop a prototype sampling system for engineering systems and reactor plant application. To complement this study, alternate techniques will be developed and evaluated. Although the vacuum distillation method has many advantages over the more widely accepted technique for impurity analyses in sodium and has demonstrated reliable oxygen analyses on sodium typical of reactor coolants, there are a number of problem areas which must be investigated to assess the over-all capabilities of the method. Of prime importance are the nature of the residues following a distillation and the effects of distillation temperatures on the nature of the residues.

The (γ,n) activation technique for the determination of carbon and oxygen in sodium has the capability for measuring oxygen specifically rather than relating the oxygen content to total alkalinity or sodium content. This method is theoretically capable of determining the concentrations of these elements directly with a sensitivity of < 1 ppm. It should provide a standard for evaluating other methods for oxygen analysis.

The development of prototype in-line analytical instrumentation for the continuous monitoring of oxygen and/or metallic impurities of interest in sodium systems is a basic requirement for the *in situ* characterization of large scale sodium systems. In-line impurity monitoring devices measure a property of sodium that is sensitive to impurity concentrations present in the flowing stream. The United Nuclear Corporation electrolytic cell and the LASL dc electrical resistivity meter which is still in its formative design stage, have both exhibited potential for in-line measurement of oxygen concentration in sodium systems. These analytical techniques must be rigorously evaluated over a range of impurity concentrations, flow, and temperature conditions in order to fully evaluate their capabilities and limitations.

B. Current Results

Operating difficulties with the dc electromagnetic pumps in the experimental facility called Analytical Loop No. 1 resulted in several shutdowns for maintenance during this reporting period. The resulting instabilities in the system caused considerable delay in the evaluation of vacuum distillation samplers. At the present time the facility has been equilibrated at an oxygen concentration of 20 ppm, corresponding to a cold trap temperature of 225°C. Sodium samples removed from the system with the full-flow vacuum distillation unit have yielded oxygen values which are in complete agreement with the results obtained with the integral vacuum distillation sampling system. The gases which are being evolved during the final stages of distillation have been analyzed by mass spectrometric techniques. Although the gases have not been positively identified they are known to be below a mass number of 40, and the volume of evolved gas is extremely minute. A gas chromatograph is being used in an

effort to identify the gases and determine their volumes.

The design of a remotely operated full-flow vacuum distillation sampling system for radioactive sodium service has been initiated. Following fabrication and operational checkout of this sampling system, it will be installed in the radioactive sodium chemistry loop of the EBR-II primary sodium system. In addition, a manually operated version of this sampling system is being developed for installation in the nonradioactive secondary sodium system of the EBR-II.

Fabrication of the Sodium Analytical Methods Facility is about 75% complete, with final assembly scheduled to start during the coming quarter. The inert-atmosphere enclosure system is ready for coupling to the distillation equipment. A sensitive gas chromatograph was installed and tested. This facility will be used for measuring the gases evolved from sodium during the distillation and from the distillation residues during subsequent analyses. Initial experiments will determine the capability of the system for low-level carbon analyses of sodium samples. This facility will be used initially to develop analytical methods for low-level (1-10 ppm) carbon analysis. After the completion of this program, it will be used to study the interaction of dissolved impurities in sodium and to identify the residues which remain after the distillation of sodium.

The engineering design drawings have been completed for the sodium sampling and transfer device which will be used in the evaluation of the (γ,n) activation analytical technique for the determination of oxygen and carbon in sodium. The mechanism will be sent out for fabrication as soon as a vendor is selected.

Atomic-absorption spectrophotometric analytical procedures are being developed for the determination of trace-level metallic impurities (other than sodium) remaining in the residue and condensate following a distillation. In addition, procedures to determine trace metallic impurities in bulk sodium samples by the same method are being investigated. An attempt is being made to run these analyses in solutions containing high concentrations of sodium ion (approximately 10%) without going through a series of chemical separations to remove sodium. Thus far, the results obtained have been very encouraging, and the method is now being used on a semi-routine basis for K, Ca, and Mg determinations.

VII. SOLUTION GETTERING

(V. J. Rutkauskas, R. R. Derusseau)

A. General

For future large sodium-cooled reactor systems, it may be desirable to use soluble getters for control of oxygen and other dissolved impurities in lieu of the more conventional hot and cold trapping techniques. The soluble metal getters of interest occur in the sodium coolant either naturally (calcium and barium), or are produced during reactor operation (as with magnesium). The techniques for the controlled additions of these getters, maintenance of fixed getter levels, and the selective removal of depleted getter metals and other impurities from dynamic sodium systems must be developed. The significant chemical reactions occurring in a sodium system containing these soluble getters must be understood and controlled. The mode of quality control using a soluble getter has the potential for effectively controlling not only oxygen, but also carbon, hydrogen, nitrogen, and possibly metallic impurities.

B. Current Results

The fabrication of components for Analytical Loop No. 2 which will be used for solution gettering studies is approximately 95% completed. The instrumentation and control cabinets have been completed. The main loop which contains the large volume sodium reservoir and the jet pump mixing chamber has been completed and assembly has been initiated on the additional sodium circuits (Fig. 2). This loop will also be used for the development and evaluation of prototype analytical instrumentation for the continuous monitoring of oxygen and/or other gaseous and metallic impurities of interest in sodium systems. The vacuum-distillation analytical technique will be employed as the primary standard in the calibration of in-line monitoring devices. In addition, experiments will be conducted to determine the lowest practical level of oxygen concentration which can be maintained in a moderately large sodium system through hot- or cold-trap modes of quality control.

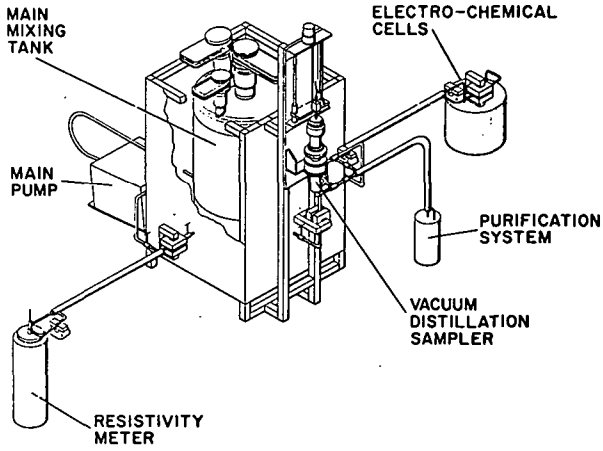

Fig. 2. Analytical Loop No. 2.

VIII. KINETICS OF SODIUM COLD TRAPS
(C. C. McPheeters, J. C. Biery)

A. General

The operation of large sodium systems requires a satisfactory method of impurity concentration control. In the absence of refractory metal structural components in high temperature regions, the use of cold traps for this impurity control may be satisfactory. The purpose of this study is to determine the mass transfer coefficients for the removal of impurities (primarily oxygen) from sodium by cold trapping. Knowledge of these coefficients will allow accurate cold trap design for cleanup of impurities and prediction of the disposition of impurities within the cold trap.

Attempts are being made to determine mass transfer coefficients by observing cleanup rates in a sodium system by cold traps of simple geometries. These cold traps are operated at various temperatures and flow rates to determine the effect of these variables on the mass transfer coefficients. The test system is an isothermal, forced-convection loop containing vacuum-distillation apparatus, a plugging indicator, and two United Nuclear Corporation oxygen meters for determination of oxygen concentration in the sodium.

The first cold trap design consists of three concentric tubes (Fig. 3). The outer annulus carries NaK which removes heat from the cold trap. Sodium flows down the inner annulus where it is cooled and up the central tube where it is reheated. A notable feature of this design is the absence of any form of packing. The packing was omitted in

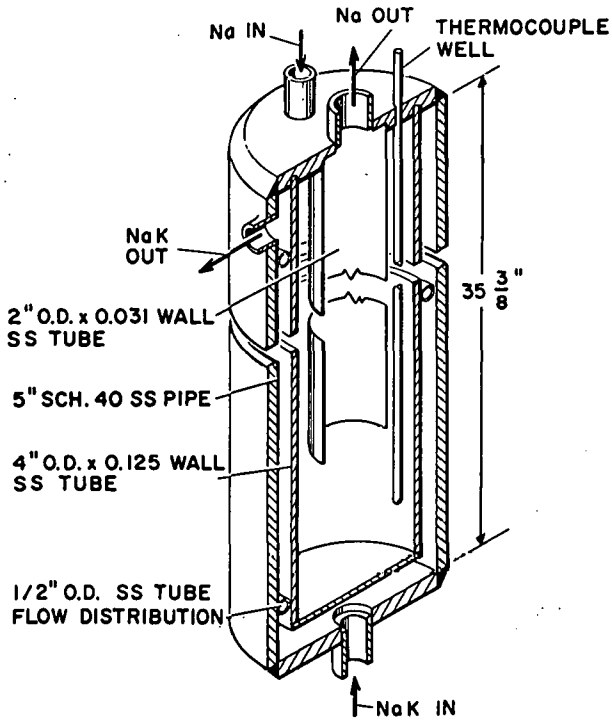

Fig. 3. Experimental Cold Trap No. 1.

order to provide a simple surface area on which the oxide could precipitate. Packed cold traps will, of course, be tested during this study.

Cold trap test runs consist of a four-day equilibration period at the initial temperature followed by a rapid change to the new temperature and flow rate. Oxygen concentration data are taken at small time intervals with all the available analytical techniques until the system concentration reaches the new equilibrium level. The resulting oxygen concentration data as a function of time are then used to determine the mass transfer coefficients.

B. Current Results

A total of eleven cold trap test runs have been completed with the first cold trap design. As shown in Table I, these runs have covered a range of sodium flow rates and cold trap temperatures.

The concentration data from each run were changed to dimensionless fractional concentrations by calculating the quantity $(C - C_e)/(C_o - C_e)$, where C_o and C_e are initial and final oxygen concentrations in the sodium and C is the concentration at any time. This quantity was plotted vs time for

Table I

Description of Test Runs with Cold Trap No. 1

Run Number	Minimum Cold Trap Temp (°C)	Flow Rate (gpm)	Initial Oxygen Concentration (ppm)	Final Oxygen Concentration (ppm)	Mass Transfer Coefficient (g/cm^2-h-ppm)
1.1		Insufficient data for proper analysis			
1.2	213	1.05	4.4	14.0	8.4*
1.3		Insufficient data for proper analysis			
1.4	180	1.0	41	5.7	27.6
1.5		Insufficient data for proper analysis			
1.6	186	0.95	42	6.9	28.4
1.7	180	0.25	58	5.7	4.5
1.8	142	0.5	42	2.2	14.3
1.9	160	0.5	48	3.3	16.6
1.10	171	0.1	43	4.4	1.26
1.11	196	0.1	46	9.1	1.23

*Mass transfer coefficient for dissolution of oxide from the cold trap. Other values are for precipitation of oxide in the cold trap.

each run. The results of these data plots for runs 1.1, 1.4, 1.6, and 1.7 are shown in Figs. 4, 5, 6, and 7. The round data points represent plugging indicator data, and the triangular points in run 1.4 represent oxygen meter data.

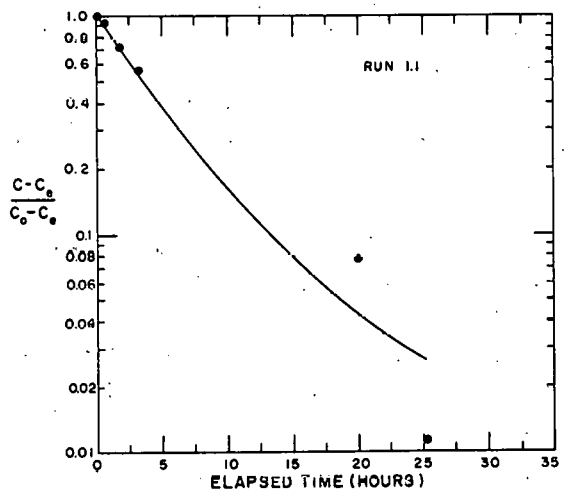

Fig. 4. Results of run 1.1. The data points are corrected plugging indicator data. The curve represents the theoretical equation with a mass transfer coefficient, K = 19.9 g/cm^2-h-ppm.

Plugging temperatures during these runs were found to be 15° to 35°C lower than the saturation temperatures based on distillation data and the LASL oxygen solubility curve. However the plugging temperatures were reproducible, and calibration of plugging temperature against distillation data allowed the plugging indicator to be used as an analytical device to concentrations as low as 5 ppm oxygen. The accuracy of the LASL solubility curve was not questioned because the equilibrium system concentration in all cases agreed quite well with that expected from the minimum cold trap temperature.

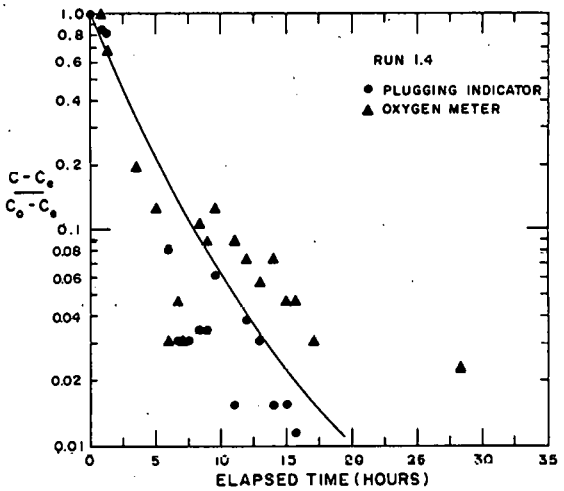

Fig. 5. Oxygen meter and corrected plugging indicator data from run 1.4. The curve represents the theoretical equation with K = 51.6 g/cm^2-h-ppm.

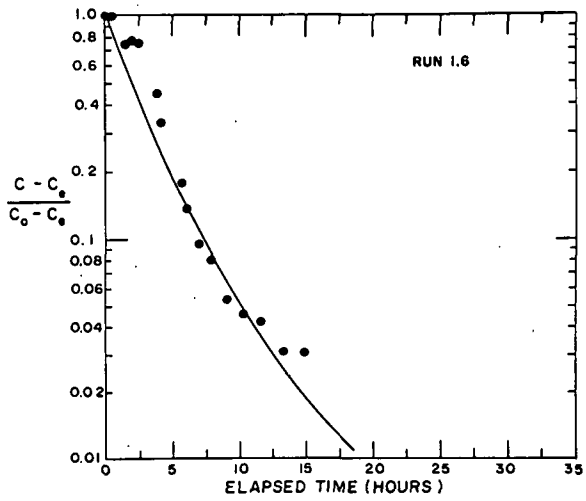

Fig. 6. Corrected plugging indicator data from run 1.6. The curve represents the theoretical equation with K = 51.2 g/cm^2-h-ppm.

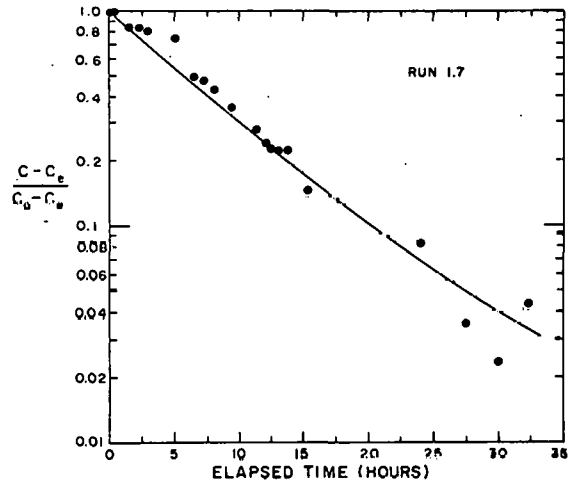

Fig. 7. Corrected plugging indicator data from run 1.7. The curve represents the theoretical equation K = 15.8 g/cm^2-h-ppm.

The precipitation rate constants are determined from Eq. 1.

$$-t = \frac{2\,\Delta M}{K} \ln \frac{A_o/\Delta + \ln(C - C_e)}{A_o/\Delta + \ln(C_o - C_e)} + \frac{M}{W} \ln \frac{C - C_e}{C_o - C_e} \quad (1)$$

where t = time, h. A_o and Δ are constants which depend on the cold trap temperature distribution.

M = sodium system mass, g.

K = precipitation rate constant, g/cm^2-h-ppm.

C = system concentration at any time, ppm.

C_o = initial system concentration, ppm.

C_e = final system concentration, ppm.

W = sodium flow rate, g/h.

Experimental data from these runs indicate that the rate constants are functions of temperature and flow rate. The temperature dependence follows a typical Arrhenius relationship with an activation energy for precipitation and dissolution of approximately 12,000 cal/mole. The dissolution rate constant was a factor of 100 lower than the precipitation rate constant when compared at the same temperature. The relationship between sodium velocity and the precipitation rate constant followed the expected proportionality with the rate constant approximately proportional to velocity to the 0.8 power. (The exception to this was the data from the 0.5 gpm runs. In these cases, the rate constant was much higher than expected.)

Additional runs will be made with this cold trap design to further define the rate constants. Packed cold traps will then be run to determine the applicability of these rate constants to this type of system.

IX. BASIC STUDIES

1. Correlation of Sodium and Helium Leak Rates (D. C. Kirkpatrick, J. P. Brainard)

A. General

The correlation of sodium leak development with measured helium leak rates provides information on the degree of component integrity which must be attained for safe long-term sodium plant operation. There are no firm criteria now in existence which establish acceptable levels of tightness for various situations.

This study uses fabricated stainless steel leaks with a range of helium leak rates. Each of these leaks will be incorporated into a small sodium system which will be held at a predetermined temperature until sodium leakage occurs.

B. Current Results

An initial experiment involving two small sodium systems with leaks fabricated by tube compression is being prepared. One leak is a large one: 2 x 10^{-4} atm-cc He/sec. The other leak is less than 10^{-10} atm-cc He/sec. These leaks should give maximum and minimum effects. A stainless steel reaction chamber filled with air at STP will be placed around the

leak to simulate real leak situations. A mass spectrometer at room temperature will sample the reaction chamber gas periodically. Although sodium or sodium oxide will probably not be detected with the room temperature mass spectrometer, a sodium leak should be observed by the decrease in oxygen in the air. Less than one milligram of sodium will react with all the oxygen in one standard cubic centimeter of air. The reaction chamber, therefore, will be less than 10 cc for the sake of safety. The temperature controllers for the sodium systems have been completed.

A vacuum oven has been set up to bake out water and oil from leaks which are known to be present in bar stock samples. Also, the effect of temperature on mass spectrometer components can be studied in this oven. The oven is made of stainless steel and has an 8.5-liter working volume. The maximum temperature attainable is greater than 700°C with existing power supplies.

2. Diffusion of Gases in Metals
(J. P. Brainard)

A. General

Very little quantitative information is available on the diffusion of gases in reactor system containment materials, although this phenomenon is known to occur in high-temperature liquid-metal-cooled systems. By use of ultra-high vacuum techniques and a mass spectrometer residual gas analyzer, diffusion rates of 1×10^{-11} to 1×10^{-12} torr-liter/sec-cm^2 (about 1×10^{-13} to 1×10^{-14} g/sec) equivalent nitrogen should be easily observable by means of a pressure change in a fixed volume.

B. Current Results

The steady-state condition for a gas flow into an evacuated work volume is PS = Q, where P is the pressure in the volume, S is the pumping speed, and Q is the flow. A work volume with a small pumping speed and a pressure gauge capable of reading small pressures are necessary for the small flows expected from the diffusion of gases through metals.

The problem with such a system is that the gauge sensitivity for low pressure measurements and the small pumping speed are known to change significantly over the long periods of time which will be needed for the diffusion studies. These changes result mainly from the reaction of gases with the system. Thus, the system must be continually calibrated during the diffusion experiments to obtain accurate results. A method of periodically injecting a known flow and observing the response of the flow measurement system is being considered.

X. COVER GAS ANALYSIS
(C. R. Winkelman, J. P. Brainard)

A. General

Cover gas analyzers for high-temperature sodium-cooled reactors must be capable of detecting impurities such as nitrogen, oxygen, hydrogen, carbon dioxide, and methane in the cover gas with a sensitivity adequate to measure these impurities from the part-per-million range to the percent range. The analyses should be accurate to at least 5% and reproducible to about 1%. High-temperature on-line operation would be necessary to prevent absorption of sodium compounds and fission products on the walls of the apparatus.

A prototype analysis system has been constructed with which to investigate the special needs of 500°-600°C cover gas analysis apparatus. The prototype includes a wide-range bakeable quadrupole mass filter residual gas analyzer. Design techniques used in the prototype are representative of those required for a 500°-600°C system.

B. Current Results

A capacitance manometer for precise measurement of the sample system pressure was installed in the mass spectrometer and all low temperature components were removed from inside the oven.

Exposure of the mass spectrometer to sodium systems is a concern. The corrosive sodium can be eliminated by such methods as condensation or surface ionization. The question is whether this is necessary in the cover gas analysis. A gas analysis of a sodium distillation loop with a sector mass spectrometer at room temperature indicated no sodium or sodium oxide. Apparently, the sodium condenses on the cool walls of the mass spectrometer. Further exposures of mass spectrometers to sodium systems will be done.

Sensitivity of the quadrupole mass spectrometer has been found to be a strong function of temperature. The electron multiplier is believed to be the main source of this variation. A study of

this effect is necessary in order to avoid recalibration when the temperature is changed.

REFERENCES

1. D. B. Hall et al., "Quarterly Status Report on the Advanced Plutonium Fuels Program, October 1 - December 30, 1966," Report LA-3650-MS, Los Alamos Scientific Laboratory, January 24, 1967.

PROJECT 807

CERAMIC PLUTONIUM FUEL MATERIALS

Person in Charge: R. D. Baker

Principal Investigator: J. A. Leary

I. INTRODUCTION

The principal goals of this project are to prepare pure, well characterized plutonium fuel materials, and to determine their high temperature properties. Properties of interest are (1) thermal stability, (2) thermal expansion, (3) thermal conductivity, (4) phase relationships by differential thermal analysis, (5) structure and phase relationships by x-ray diffraction, high temperature x-ray diffraction, neutron diffraction and high-temperature neutron diffraction, (6) density, (7) hardness and its temperature dependence, (8) compatibility including electron microprobe analysis, (9) compressive creep (deformation).

In addition to phase equilibria and general properties, specific thermodynamic properties such as free energy of formation by vaporization equilibria in the 1000-2000°C temperature range with mass spectrometer identification of vapor species, free energy of formation by electromotive force measurement in the 450-1200°C temperature range, and heat capacity and heat of transition are being determined.

II. SYNTHESIS AND FABRICATION

(M. W. Shupe, R. L. Nance)

1. Carbides

Approximately 1 cm dia pellets of $U_{0.8}Pu_{0.2}C_{1-x}$, $U_{0.8}Pu_{0.2}C_{1+x}$, $U_{0.8}Pu_{0.2}C$, $U_{0.9}Pu_{0.1}C_2$, $U_{0.8}Pu_{0.2}C_2$, and $U_{0.5}Pu_{0.5}C_2$ were prepared for thermal analysis. Pellets of $U_{0.8}Pu_{0.2}C_{1.5+x}$ also were prepared for use as electrodes in electromotive force measurements. In addition, $U_{0.8}Pu_{0.2}C_{1.5+x}$ and $PuC_{1.5+x}$ pellets were synthesized for analytical chemistry development.

2. Hydrogen Reduction of $(U, Pu)_2C_3/(U, Pu)C_2$ to (U, Pu)C

In the previous report the possibility of an H_2 reduction method to prepare large amounts of single phase (U, Pu)C powders was discussed. The effects of several process variables, such as reaction time, particle size and the planar area of the powder boat were examined. Process variables held constant during these examinations were the initial C/M ratio, the graphite electrode, the H_2 flow rate of 0.5 ℓ/min. and the reaction temperature of 850°C. The initial results, which were accomplished using a furnace with a ceramic core, a small boat and -325 mesh powder are shown in Table 807-I.

These tests indicated that a nearly complete reduction of M_2C_3 to MC could be routinely attained under the described conditions. This was later confirmed.

A second series of evaluations has been accomplished using a stainless steel tube in place of the ceramic tube, and a larger W boat having a planar area of 49 cm^2. The results of reduction at a rate of 0.4 hr/g are shown in Table 807-II.

Table 807-I

Effect of Reaction Time on Hydrogen Reduction

(ceramic core, small reaction boat)

Lot No.	C/M Ratio			v/o M_2C_3 in Pellet Microstructure		
	Initial	0.4 hr/g	0.8 hr/g	Initial	0.4 hr/g	0.8 hr/g
9-151-1	1.001	0.981	0.981	0.10	> 0.5	0
9-143-2	0.994	0.978	0.976	0.15	> 0.5	0
6-2-1	...	0.990	...	0.20	1	...
6-4-1	1.035	0.981	...	0.20	1	...

Table 807-II

Hydrogen Reduction of $(U, Pu)_2C_3$ in $U_x Pu_y C_z$ Powders

(Reaction time: 0.4 hr/g)

Lot No.	Initial			Reduced			Particle Size,	Pellet Microstructure[1]
	x	y	z	x	y	z	μ	
6-44-1	0.793	0.208	1.009	0.794	0.206	0.971	≤ 44	MC, P
6-44-2	0.800	0.200	0.996	0.800	0.200	0.974	≤ 44	MC, P
6-47-2	0.796	0.202	0.998	0.795	0.205	0.942	≤ 74	MC, I
6-53-1	0.796	0.204	0.978	0.795	0.205	0.984	≤ 74	MC
6-53-2	0.799	0.201	1.050	0.798	0.202	0.988	≤ 74	MC

Note: (1) P = platelets, I = metallic impurity, ≤ 0.5 v/o

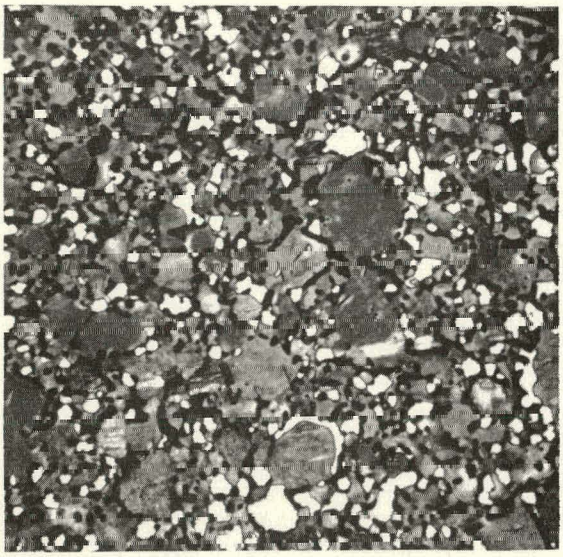

Fig. 807-1 Hyperstoichiometric UC lot 6-29-1 Before H_2 Reduction (Nitric-Lactic-Acetic etch; 380X)

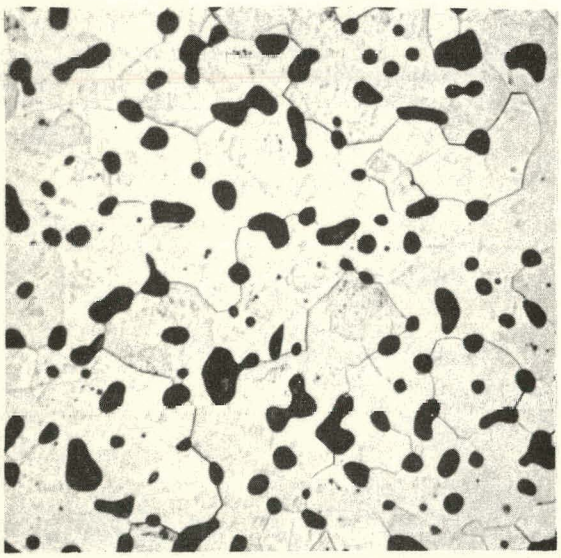

Fig. 807-2 Single Phase UC lot 6-29-1 After H_2 Reduction (Nitric-Lactic-Acetic etch; 380X)

The pellets from lot 6-44-1 that contained the dicarbide-type platelets in the microstructures were retreated for 16 hr at 850°C in flowing H_2. This treatment eliminated all of the dicarbide, and most of the sesquicarbide.

Depleted UC pellets are required to serve as thermal insulators at each end of each (U, Pu)C - loaded pin for the EBR-II irradiations (see project 808). Therefore the H_2 reduction treatment was also tested on UC_{1+x} lot 6-29-1. The reduction of U_2C_3 is shown in Figures 807-1 and 807-2.

3. Oxides

Several lots of $U_{0.8}Pu_{0.2}O_2$ powder are being prepared to be used as analytical chemistry intermediate reference standards as part of a cooperation program with the New Brunswick Laboratory. Six 35 g lots of varying purity and varying Pu/U ratio from 5/95 to 30/70, and one 200 g lot having the ratio Pu/(U + Pu) = 20.0 percent by wt. are required. The conventional ADU-$Pu(OH)_4$ coprecipitation procedure has been used, followed finally by high temperature firing of the powder in wet H_2 ($H_2O/H_2 = 10^{-2}$) at 1550°C. Present status is that the six small lots are completed, while the large lot has been completed up to the point of firing at 1550°C. The chemical composition of the 200 g lot is shown in Table 807-III. The lattice dimensions of the high-fired small lots shown in Table 807-IV indicate uniform solid solutions are produced that follow Vegard's law. If the variation of lattice dimension with O/M ratio indicated in GEAP-4931 is correct, the lattice dimension of the (nominal) 20 percent PuO_2 composition indicates an O/M ratio of 2.014 for this sample.

Relative rates of solution of $U_{0.8}Pu_{0.2}O_2$ before and after firing at 1550°C have been determined. The low fired powder had been heated in H_2 at 925°C to reduce U_3O_8 to UO_2. As anticipated, the high fired powder dissolved more readily than the low fired material, presumably because of solid solution formation at the high temperature. After 2 h in hot 15 M HNO_3, 99.4 % of the high fired material had dissolved, in comparison to 88.9 percent of the low fired material. All residues were dissolved completely by fuming with a $HF-HNO_3-H_2SO_4$ mixture.

Table 807-III

Spectrochemical Analysis of $(U, Pu)O_2$

(200 g lot)

Element	$g/10^6$ g Pu
Li	< 1
Be	< 1
B	10
Na	5
Mg	5
Al	< 10
Si	55
P	< 50
Ca	< 5
Ti	< 50
V	< 5
Cr	< 10
Mn	< 2
Fe	< 20
Co	< 5
Ni	< 10
Cu	5
Zn	< 10
Sr	< 5
Y	ND
Zr	< 100
Nb	< 50
Mo	< 10
Cd	< 10
Sn	10
Ba	< 10
Ta	<1000
W	< 10
Pb	< 2
Bi	< 2

Table 807-IV

Lattice Dimensions of $(U, Pu)O_2$ Powders
Heated to 1550°C in Wet H_2

Pu Conc., (g Pu × 100/g(U+Pu))	Lattice Parameter, A
0	5.4691
4.58 ± 0.01	5.4663
10.39 ± 0.01	5.4619
16.09 ± 0.01	5.4579
20.80 ± 0.02	5.4541
24.78 ± 0.02	5.4513
31.12 ± 0.02	5.4468
(100% PuO_2)	5.3950

III. PROPERTIES

1. Differential Thermal Analysis
(J. G. Reavis, C. W. Baker)

Determination of solidus and liquidus temperatures of U-Pu-C compositions by DTA and metallographic techniques is continuing. Preliminary observations also have been made in determining of the heat of fusion of UO_2-PuO_2 solid solutions by DTA.

Melting of (U, Pu)C: In previous reports solidus and liquidus temperatures for $U_{0.8}Pu_{0.2}C$ as determined by DTA were given as 2325 ± 50° and 2475 ± 50°, respectively. Additional observations have been made to refine the precisions of these values.

Two lots of carbide pellets have been thermally cycled, and DTA observations have been compared with the microstructures of these heat treated pellets. Each pellet was heated at 30 to 100°C/min., held at equilibration temperature for 1 min., then quenched to 1000°C at 1000°C/min. Thereafter the pellets were cooled to room temperature within a few minutes, then examined. All pellets used in these experiments had previously been sintered at 1600°C.

Effects of this treatment on carbide microstructure are shown for two carbide compositions in Figure 807-3. The $U_{0.81}Pu_{0.19}C_{0.95}$ sample initially contained < 1 percent by volume of a second metallic phase. The metallic impurity phase contained Pu, U, W, Si, and Fe. Photomicrographs of samples quenched from 2200° and 2225° do not show the presence of this phase, while a sample cooled slowly from 2200° (not shown) had reverted to the 1600° appearance. The 2250° photomicrograph shows the first evidence of what is believed to indicate melting. Both electron microprobe analysis and metallographic etching tests indicate that the unstained grain boundary regions and the regions around pores are carbide but also are enriched in Pu, thus indicating melting followed by coring during resolidification. The 2465° sample had (by macro observation) almost completely melted. Other macro and DTA observations show that the liquidus temperature is 2475 ± 25°C. Thus, the solid plus liquid region of $U_{0.81}Pu_{0.19}C_{0.95}$ appears to be from 2250 to 2475°C.

The composition of the pellets used in the second series shown in Figure 807-3 was found by chemical analysis to be $U_{0.81}Pu_{0.19}C_{0.99}$. The 1600° photomicrograph shows that "MC_2 platelets" and small areas of

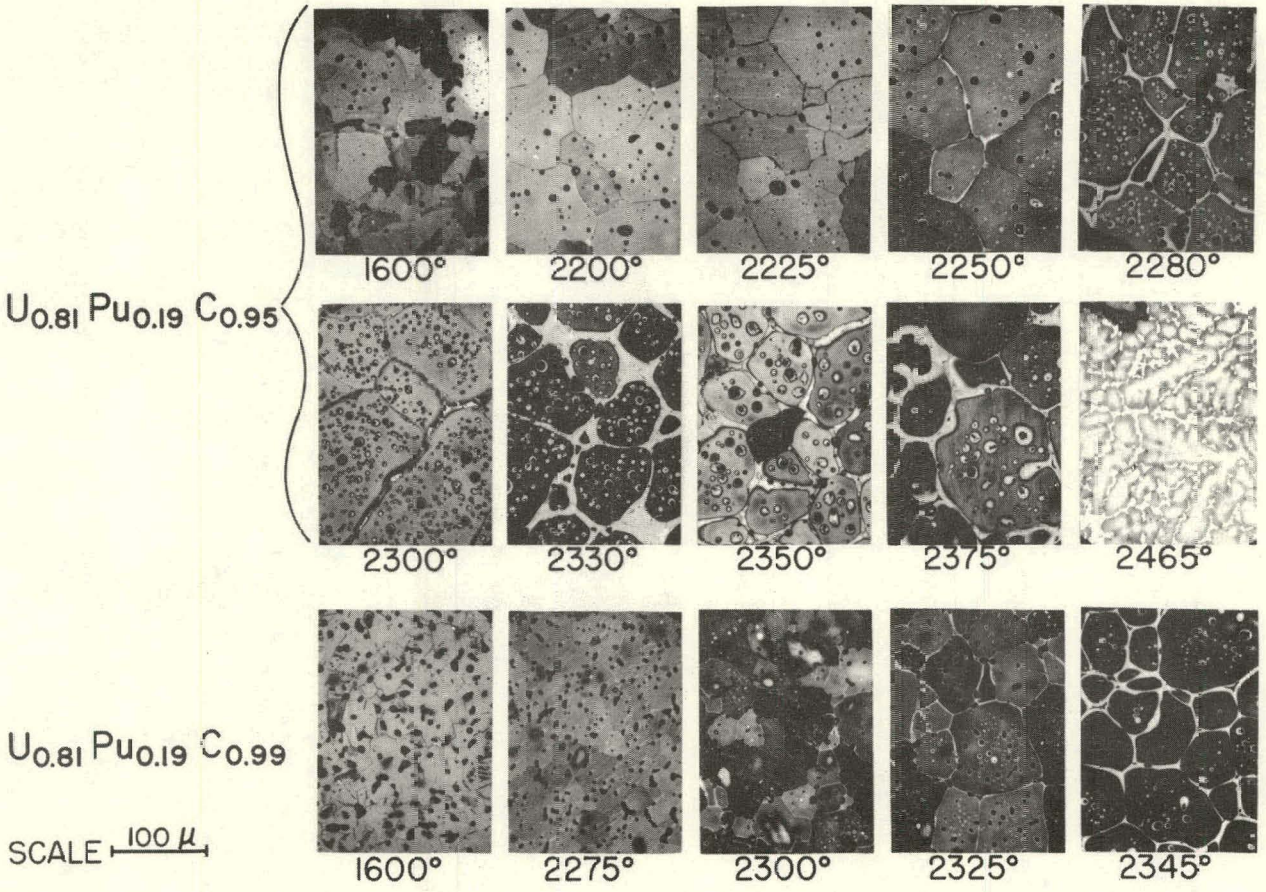

MELTING BEHAVIOR OF U, Pu MONOCARBIDES

(SPECIMENS HELD FOR 1 MIN. AT TEMP. UNDER Ar)

Fig. 807-3

M_2C_3 were present in the sintered material. Observations similar to those outlined in the preceding paragraph lead to the conclusion that the solid to liquid range of $U_{0.81}Pu_{0.19}C_{0.99}$ is from 2300 to 2485°C.

The results of this series of observations tend to support the previously reported liquidus temperatures determined by DTA, but also indicate that solidus temperatures determined by DTA alone may be somewhat high.

Heat of Fusion of UO_2-PuO_2: DTA techniques are being developed for determinating the heat of fusion of LMFBR fuel materials. As part of a cooperative program with GE-Sunnyvale, samples of ZrO_2 and of UO_2-20% PuO_2 in sealed W capsules have been cycled through their respective melting points and a preliminary estimate of the heat of fusion of UO_2-20% PuO_2 has been made. This preliminary value is 23 ± 5 kcal/mole, based on a value of 20.8 kcal/mole for the heat of fusion of ZrO_2 which is being used as a reference material. Additional samples have been sealed in W capsules to allow determination of the reproducibility of the method and to reduce the uncertainty in the actual value of the heat of fusion.

The observed melting point of ZrO_2 was 2700 ± 20° (literature value 2710 ± 10°)[1] and the temperatures of UO_2-20% PuO_2 were observed to be 2775° and 2815°, respectively, as compared to 2760° and 2790° reported by Lyon and Baily.[3]

2. X-ray Powder Diffraction
(C. W. Bjorklund, R. M. Douglass, R. L. Nance)

Work is continuing on x-ray powder diffraction studies of various uranium-plutonium fuel materials, most of which has been reported in other sections. Additional data have also been obtained in the study of self-irradiation damage in plutonium ceramics as a function of time, temperature and dose. The lattice expansion caused by self-irradiation damage in Pu_2C_3 of normal isotopic composition continues at an almost linear rate after more than 800 d. Similar results were reported previously for samples of PuN and PuO_2 of normal isotopic composition observed for periods of 1350 and 1500 d, respectively. On the other hand, the lattice expansions of plutonium compounds enriched with ^{238}Pu have all apparently attained saturation values in less than 600 d which is equivalent to about 6,000 d for normal isotopic compositions. The latter group of compounds includes $PuC_{0.86}$ and duplicate samples of PuC and Pu_2C_3 in a two-phase equilibrium system, all containing 4.05 a/o ^{238}Pu, and duplicate samples of PuO_2 (containing 3.75 a/o ^{238}Pu) stored at -198°, 25°, 100°, 200° and 400°C. As was noted in the previous quarterly report the lattice dimension of the PuC phase in equilibrium with Pu_2C_3 has been following an apparent cyclical oscillation about an average maximum value which still continues. This oscillation appears to be real despite the greater uncertainties in measurement caused by line broadening and increased background in the back reflection region. The PuC-Pu_2C_3 two-phase system was the only one for which significant line-broadening was observed as radiation damage increased. Reflections attributable to a Pu_2C_3 phase have recently been detected on films obtained for the originally single phase $PuC_{0.86}$ sample. Increased background intensity has also been observed on these films, but no significant line-broadening has been detected. No deterioration in line quality or background intensity has been observed on films of the other compounds.

When the relative lattice expansion of all of the compounds under study were plotted as a function of the accumulated dose instead of time, only the data for normal and enriched samples of PuO_2 fell on the same curve. The accumulated dose is the product of the elapsed time and an average disintegration constant calculated from the disintegration constants and relative amounts of the Pu isotopes in each compound.

A non-linear least squares computer program has been used to calculate the parameters in the equation relating lattice expansion to time, namely:

$$a_t = P_1\left(1-e^{P_2 t}\right) + a_o \qquad (1)$$

where a_t is the measured lattice dimension at time t, and P_1, P_2 and a_o are the parameters to be calculated. a_o is the calculated value of the lattice dimension at

time 0. This program has been modified to fit the equation

$$a_t = \left(\frac{A_1}{T} + A_2\right)\left[1 - e^{t\left(\frac{A_3}{T} + A_4\right)}\right] + a_o \qquad (2)$$

where a_t, t and a_o have the same significance as in Eq. (1). Equation (2) was derived from Eq. (1) to fit the data obtained for the samples of enriched PuO_2 stored at -198°, 25°, 100°, 200°, and 400°C. It was obtained by substituting the expressions $\left(\frac{A_1}{T} + A_2\right)$ and $\left(\frac{A_3}{T} + A_4\right)$ for P_1 and P_2, respectively, in Eq. (1). T, in these expressions, is the temperature in degrees Kelvin at which each sample was stored. Least squares values of A_1 through A_4 and a_o were calculated by the computer program. P_1 and P_2 were found to be strictly linear functions of $\frac{1}{T}$ only over the range 373-673°K. However, the deviation from linearity of the values obtained at 25°C was small enough that the data obtained at 25°C were included as a first approximation in the least squares calculation. Data for samples stored at -198°C could not be reconciled with the linear expressions and were omitted. The following values were obtained for the parameters in Eq. (2):

$A_1 = 3.30 \quad (\pm 0.1)$
$A_2 = 5.7_3 \quad (\pm 0.3) \times 10^{-3}$
$A_3 = 2.5_9 \quad (\pm 0.5)$
$A_4 = -2.0_5 \quad (\pm 0.1) \times 10^{-2}$
$A_5 = 5.3953 \quad (\pm 0.0001)$

These values substituted in Eq. (2) were found to reproduce the experimental data reasonably well. Modifications of the equation to provide an even better fit to the data obtained at 25° are now under study.

3. High Temperature X-ray Diffraction
(J. L. Green)

Work has continued on the high temperature furnace for the x-ray diffractometer. A technique has been developed for the preparation of samples for the furnace using NbC as a test material. Thin uniform layers of powder were loaded onto the graphite heater strip using naphthalene as a binder. These composites were then sintered in Ar to produce a thin uniform layer of NbC which was sufficiently adherent to be stable during thermal cycling. Several expansion coefficient determinations have been attempted using NbC samples. Early trials failed because of sample oxidation. However, more recent experiments were successful in that the expansion curves determined in the range 25-1800°C agreed quite well with published data. There are indications that some oxidation is still occurring at high temperatures. Work is, therefore, being done to try to eliminate the remaining sources of oxidants.

4. Neutron Diffraction
(J. L. Green)

The room temperature structure of Pu_2C_3 was first described by Zachariasen[1] in 1944. It is body centered cubic and in space group $I\bar{4}3d$ and has 8 formula weights per unit cell. The Pu ions are located in the 16 fold (c) positions and the C atoms in the 24 fold (d) positions, both of which require one positional parameter for description. Based on x-ray intensity data Zachariasen was able to define the metal parameter as 0.050 ± 0.003. Because of the small x-ray scattering amplitude of carbon relative to plutonium, he was not able to determine the anion position parameter. As in the case of PuC, Costa and Lallement[5] have suggested that a possible antiferromagnetic transition occurs in Pu_2C_3 at approximately 120°K.

In order to investigate these problems, two targets of carbon-saturated Pu_2C_3 were prepared and scanned. The early target was prepared using ^{239}Pu and was studied only at room temperature. The second was prepared using ^{240}Pu and was studied both at room temperature and at cryogenic temperatures.

A comparison of room temperature and low temperature data indicates that if a magnetic transition does occur, it was not experimentally observable.

Considerable crystallographic information on the structure can be derived from the room temperature data from both targets. Figure 807-4 is a schematic representation of the room temperature diffraction pattern for the ^{240}Pu target. Numerical intensity

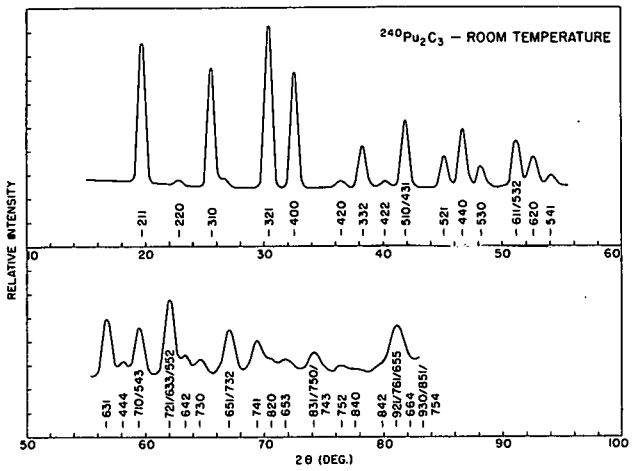

Fig. 807-4 Room Temperature Neutron Diffraction Pattern for $^{240}Pu_2C_3$

information was extracted from the counting data using a least squares Gaussian fitting computer program. For the ^{240}Pu target, it was possible to obtain data for 46 diffraction peaks. The resolution of the ^{239}Pu target was not nearly as good due to the large fast fission neutron background; however, it was possible to obtain intensity information on 12 low angle reflections. These data were then used in a computer program which calculates the various crystal parameters by least squares fitting the observed intensities. The results of these calculations are shown in Table 807-V. The recent data on U_2C_3 by DeNovion et al.[6] is shown for comparison.

Agreement between the two independent Pu_2C_3 determinations is quite good. As expected, the atomic position parameters for Pu_2C_3 and U_2C_3 are very similar. The only major difference is in the value of the thermal parameter, B. Whether or not this difference is real is somewhat difficult to determine. The value of B is rather sensitive to the accuracy of the absorption corrections and also there appears to be a rather strong correlation between the value of B and the calculated value for the instrumental constant. A quantity of interest that may be computed from these data is the C-C bond length. The carbon atoms in the Pu_2C_3 type structure occur as dicarbide groups. This bond length is 1.39 Å in Pu_2C_3 and 1.42 Å in U_2C_3. It is pertinent to point out that these are significantly longer than the value of 1.295 Å reported for U_2C_3 by Austin.[7]

Table 807-V

Pu_2C_3 CRYSTALLOGRAPHIC PARAMETERS

	$^{239}Pu_2C_3$	$^{240}Pu_2C_3$	U_2C_3
X_{Pu}	0.050 ±0.002	0.0492 ±0.0005	0.0485 ±0.0002
X_C	0.289 ±0.004	0.2896 ±0.0005	0.2872 ±0.0005
b_{Pu}	0.77 ±0.10	0.409 ±0.007	—
B(thermal)	~0.7 Å^2	0.69 ±0.06 Å^2	0.30 ±0.01 Å^2
R(intensity)	0.06	0.06	0.02
a_o	8.132 Å	8.135 Å	8.089 Å
C-C bond	1.40 Å	1.39 Å	1.42 Å

5. Thermodynamic Properties of Plutonium Compounds by Electromotive Force Techniques
(G. M. Campbell)

Nitrides: A galvanostatic technique for determining the Pu, Pu^{+3} equilibrium potential using a W microelectrode has been developed. The procedure involves electrodeposition of Pu metal from the fused salt electrolyte, onto the microelectrode by a constant current, followed by anodic stripping of the Pu metal at constant current. By recording the potential during the procedure and having a theoretical knowledge of Pu^{+3} diffusion effect on concentration at the electrode surface, the equilibrium potential can be determined. Experiments which made use of a Pu, Pu^{+3} liquid metal electrode as a reference standard, indicate the technique is probably accurate to ± 1 mv in melts of high purity. Tho purity of the melts is indicated by the residual current observed in the chronopotentiometric trace.

This galvanostatic technique has been used to determine the emf of a PuN electrode in LiCl-KCl, $PuCl_3$ melt, in the temperature range of 915 to 1031°K. The data are presented in Table 807-VI and Figure 807-5. After correcting the N_2 pressure to 1 atm and performing a least squares analysis of the data, the emf is given by

$$E = 1.043 - 0.000316\ T\ (\pm\ 0.005)\ \text{volts},$$

for the cell

$$Pu(\ell)(PuN(s))/Pu^{+3},\ LiCl\text{-}KCl/PuN(s),\ N_2(g)\ .$$

This results in a standard free energy of formation of

$$-\Delta G^{o}_{T} = 72.1 - 0.0219\ T\ (\pm\ 0.4)\ \text{kcal/mole}$$

for the reaction

$$Pu(PuN) + 0.5\ N_2 \rightarrow PuN \ .$$

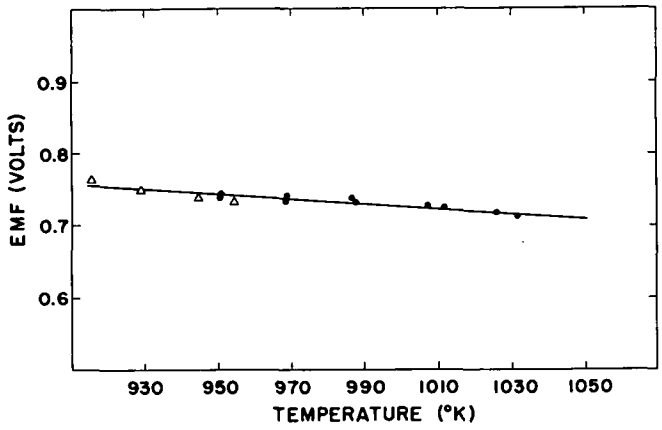

Fig. 807-5 EMF vs Temperature for the Cell Pu(ℓ), PuN(s)/Pu^{+3}, LiCl-KCl/PuN(s), N_2(g) (● = cell no. 1; Δ= cell no. 2)

Table 807-VI

EMF of Pu(ℓ) vs PuN(s), N_2(g)

Cell no.	EMF (V)	N_2 Pressure (atm)	EMF Corrected to 1 atm N_2	Temp., °K
1	0.7425	0.755	0.7380	950.1
1	0.7450	0.716	0.7404	950.1
1	0.7380	0.749	0.7340	968.5
1	0.7448	0.734	0.7405	968.1
1	0.7375	0.751	0.7334	987.2
1	0.7415	0.751	0.7374	986.2
1	0.7310	0.755	0.7269	1007.1
1	0.7210	0.755	0.7169	1025.9
1	0.7295	0.755	0.7254	1011.9
1	0.7180	0.755	0.7138	1031.6
2	0.7382	0.728	0.7338	954.2
2	0.7415	0.714	0.7369	944.4
2	0.7540	0.707	0.7494	929.3
2	0.7675	0.686	0.7626	915.6

This is to be compared with the value of -60 ± 1 kcal/mole previously obtained for the free energy of formation at 700°K.[8] Although N_2 is known to react with Pu at these temperatures and PuN formation is indicated on the chromopotentiometric trace, the cell potential can be easily corrected in order to determine the equilibrium potential. Since it is rather doubtful that PuN is soluble in Pu to a significant extent at these temperatures the cell reaction is for all practical purposes written as

$$Pu(\ell) + 0.5\ N_2(g) \rightarrow PuN(s) \ .$$

Carbides: Thermodynamic properties of PuC and Pu_2C_3 have been reported previously. One preliminary experiment was conducted on the $(U_{0.8}Pu_{0.2})_2C_3$ solid solution. A sintered pellet was used as an electrode and a $PuRu_2$ + Ru electrode was used as the reference. This system did not seem reliable due to the rather large positive polarity of the solid solution and the possibility of U transfer to the $PuRu_2$ + Ru electrode. No U was detected in the molten salt electrolyte after a 70 h equilibration, however. (The spectrophotometric analysis method used to determine U was sensitive to < 10 ppm.) The galvanostatic technique did give reasonable data for the system. However further experiments will be required before a competent assessment can be made.

6. Thermodynamic Properties from Vaporization Studies
(R. A. Kent)

The system PuN has been studied mass spectrometrically. The PuN samples were prepared by pressing pellets from PuN powder[9] having a stoichiometry of $PuN_{0.95}$ and heating these pellets under 0.5 atm N_2 at 1600° for 15 h. Metallographic and x-ray diffraction analyses indicated the resultant pellets to be single phase PuN with an average lattice parameter of $a_o = 4.9055 \pm 0.0002$ A. Chemical analyses indicated the stoichiometry to be $PuN_{0.96}$ to $PuN_{0.99}$.

Eight Knudsen effusion experiments were performed in which PuN pellets were heated in W cells over the range 1658 to 1976°K. The only vapor species observed over these samples were Pu and N_2. Metallographic and x-ray diffraction analyses indicated the residue to be single phase PuN with $a_o = 4.9055 \pm 0.0002$ A. The grain size of the material had increased, but no free Pu metal was found in the residues.

From the above observations and from the enthalpy values, obtained as described below, one concludes that in this temperature range PuN decomposes according to the reaction

$$PuN(s) = Pu(g) + 0.5\ N_2(g) \ . \qquad (1)$$

The enthalpy of the decomposition reaction was

determined by following the ion current of the $^{239}Pu^{+}$ signal as a function of temperature. The ion current data were converted to Pu partial pressure values in the usual manner from the equation

$$P = K\,(IT) \qquad (2)$$

where P is the vapor pressure of a given species, K is the machine constant, I is the ion current and T is the temperature in degrees Kelvin.

The value of K was determined in the usual manner by employing Au as a standard and correcting for ionization cross sections,[10] multiplier gains and threshold energies.

In the temperature range covered the partial pressure of Pu above PuN(s) is given by

$$\log_{10} P_{Pu}(atm) = (6.436 \pm 0.055) - \frac{21,953 \pm 98}{T\,^{o}K} \quad . \qquad (3)$$

Vapor pressure data for the first three experiments conducted in this investigation are shown in Figure 807-6 together with values measured[11] or estimated[12] by other workers.

For the reaction given by Eq. (1) the N_2 partial pressure is given by

$$P_{N_2} = 0.5\, P_{Pu} \left(\frac{M_{N_2}}{M_{Pu}}\right)^{0.5} = 0.171\, P_{Pu} \qquad (4)$$

where M is the molecular weight of a given species. The equilibrium constant for the dissociation reaction is given by

$$K = P_{Pu}\, P_{N_2}{}^{0.5} = 0.4135\, P_{Pu}{}^{1.5} \qquad (5)$$

These results can be combined with the heat capacity of PuN[5] to calculate the thermodynamic functions of PuN. Because the heat capacity of PuN has not been determined, it was estimated from the heat capacity of UN.[13] The resulting free energy functions are shown in Table 807-VII.

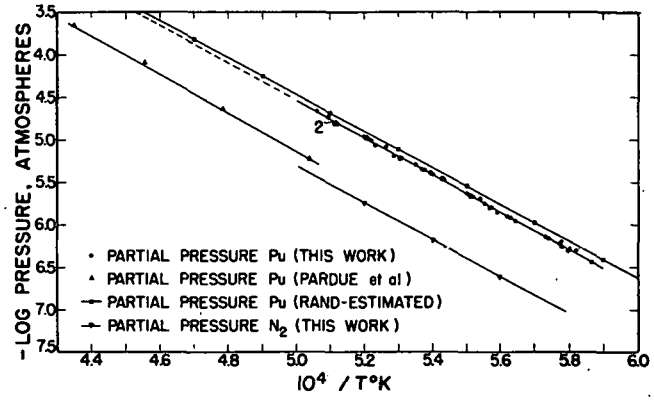

Fig. 807-6 -Log Pressure vs 1/T for PuN

Table 807-VII

Thermodynamic Functions for PuN(s)

Temp. °K	C_P^o e.u.	$H_T^o - H_{298}^o$ cal. mole^{-1}	S_T^o e.u.	$-(F_T^o - H_{298}^o)/T$ e.u.
298	12.44	0	16.30	16.30
300	12.44	22	16.48	16.41
400	12.72	1257	19.93	16.79
500	13.05	2501	22.71	17.71
600	13.39	3778	25.03	18.73
700	13.77	5102	27.07	19.78
800	14.19	6474	28.91	20.82
900	14.62	7901	30.58	21.80
1000	15.09	9382	32.14	22.76
1100	15.56	10918	33.61	23.68
1200	16.08	12512	35.00	24.57
1300	16.61	14164	36.32	25.42
1400	17.17	15908	37.58	26.22
1500	17.73	17641	38.80	27.04
1600	18.33	19465	39.98	27.81
1700	18.94	21349	41.12	28.56
1800	19.56	23289	42.23	29.29
1900	20.22	25290	43.21	30.00
2000	20.88	27349	44.23	30.66
Estimated Error at				
298	3%	—	5%	5%
2000	30%	15%	15%	15%

Equation (3) leads to an enthalpy of reaction 1 of

$$\Delta H_{1813} = 150.7 \pm 0.6 \text{ kcal. mole}^{-1} \quad .$$

when this value is corrected to 298°K, using values of $(H_T^o - H_{298}^o)$ for PuN from Table 807-VII, and tabulated values for Pu(g)[14] and N_2(g)[15] the second law decomposition enthalpy becomes

$$\Delta H_{298}^o = 156.2 \pm 0.8 \text{ kcal. mole}^{-1} \quad .$$

When the values of the equilibrium constant calcu-

lated from the Pu partial pressure data according to Eq. (5) are combined with the free energy functions for PuN from Table 807-VII and for Pu(g) and N_2(g) the resultant third law value of the decomposition enthalpy is

$$\Delta H^{o}_{298} = 156.1 \pm 0.2 \text{ kcal. mole}^{-1} .$$

The errors quoted in the enthalpy values and in Eq. (3) are the standard deviations generated by a least squares fit to the data. The true uncertainties may be larger due to errors in temperature measurement, the ionization cross section values employed, and in the estimated values of the thermodynamic functions employed for PuN. Accordingly the decomposition enthalpy was taken to be

$$\Delta H^{o}_{298} = 156.1 \pm 2.5 \text{ kcal. mole}^{-1} .$$

When this value is combined with the enthalpy of vaporization of Pu metal, $\Delta H^{o}_{298} = 83.0 \pm 0.5$ kcal. mole^{-1}, the standard enthalpy of formation of PuN(s) is calculated to be

$$\Delta H^{o}_{298} = -73.1 \pm 2.6 \text{ kcal. mole}^{-1} .$$

7. Iligh Temperature Calorimetry
(A. E. Ogard)

The high temperature heat contents and heat capacities of $U_{0.8}Pu_{0.2}O_2$ and $U_{0.8}Pu_{0.2}O_{1.98}$ are being determined as part of a cooperative program with GE-Sunnyvale. In addition, these properties are being determined for UO_2 and α-Al_2O_3. To date the measurements have been completed up to ~ 2300°K in a drop calorimeter that was not enclosed in a glovebox. At these high temperatures, grain growth is extensive in the welds of the W capsules used to contain the oxides. Therefore the calorimeter has been relocated in a plutonium handling enclosure, and the calorimeter is being recalibrated. It has been demonstrated that in the new assembly, calibration is independent of the rate heat input over the range 700 to 2,000 cal/min., and independent of the integral heat input over the range 1,000 to 15,000 cal. The calibration factor has been improved to a precision of ± 0.2 percent, which appears to be the practical limit.

IV. ANALYTICAL CHEMISTRY

1. Spectrochemical Determination of Impurities in U-Pu Ceramic Type Fuel Materials
(W. M. Myers, C. B. Collier, R. T. Phelps)

Spectrochemical methods are being developed for determining impurities in mixed carbides, mixed nitrides and mixed oxides of uranium and plutonium. A carrier-distillation technique involving the use of 6.4 percent Ga_2O_3 as a carrier and Co as an internal standard has been developed to apply to either of the above materials after the sample has been converted to the oxide by ignition. Determination of the following 21 impurities in the nominal range of 1 to 1000 ppm is accomplished: Li, Be, B, Na, Mg, Al, Si, P, Ca, Cr, Mn, Fe, Ni, Cu, Zn, Sr, Cd, Sn, Ba, Pb and Bi. Additional impurities are determined by a second carrier distillation technique which involves the use of 50 percent AgCl as a carrier. These are, Ti, V, Co, Zr, Nb, Mo, Ta and W.

The impurity metals most commonly found in experimental materials to date (Al, Cr, Fe, Mn, Ni, Si, and W) are evaluated by photometry with a precision of 20 percent relative standard deviation. Evaluation of concentrations by visual comparison is usually done faster but with a precision of 50 percent relative standard deviation.

The determination of additional impurities is being studied.

2. The Determination of Uranium and Plutonium in Their Mixed Carbides, Mixed Nitrides, and Mixed Oxides
(G. B. Nelson, K. S. Bergstresser and G. R. Waterbury)

Interest in determining U and Pu in these materials without prior chemical separation has resulted in applications of a controlled-potential coulometric and a potentiometric titration method to the problem. It was previously reported that for "synthetic" solutions these methods were unbiased and relative standard deviations of 0.3 percent for the coulometric method and 0.05 percent for the potentiometric method were obtained. In the analysis of (U, Pu)C, however, it was observed that a small amount of W caused interference in the potentiometric method but not in the coulometric

method. Repeated measurements showed that the 1σ precision of the potentiometric method for a W free (U, Pu)C material is 0.09 percent for U and 0.18 percent for Pu. A new transistorized controlled potential coulometer is being calibrated for use in these measurements.

3. The Gravimetric Determination of Oxygen to Metal Ratios in Uranium-Plutonium Dioxide Fuel Material
(J. W. Dahlby)

The gravimetric method reported by Lyon (GEAP Rpt. 4271, 1963) could not be made to produce satisfactory results when used according to recommendations. No combination of parameters could be found that would produce satisfactory results using pure UO_2 as the experimental material. In all cases the O/M ratio was high, between 2.006 and 2.008. It was observed, however, that the weights of the UO_2 products increased when stored overnight in a vacuum desiccator, but the increase was only enough to bring the O/M ratio down to approximately 2.004. For this reason a thermobalance is being set up to permit weighings at temperature and without removal from the He-H_2 reducing atmosphere.

4. Gravimetric Determination of Oxygen in $(U, Pu)O_2$
(C. S. MacDougall and M. E. Smith)

Using ThO_2 as a stand-in for $(U,Pu)O_2$ a gravimetric method for determining oxygen was found to have a precision of 0.4 percent relative standard deviation. All attempts to improve this figure failed. Attempts are now being made to apply an inert-gas-fusion technique by using a molten metal bath and an automatic temperature programmer.

5. Gas Chromatographic Determination of Oxygen in $(U, Pu)O_2$
(M. E. Smith and D. Vance)

An inert-gas-fusion gas chromatographic finish method for measuring oxygen in these materials is being tested. The CO and CO_2 liberated at 2,000°C from an oxide fuel-C pellet are mixed with ethane as an internal standard and measured in a gas chromatograph. Although the CO can be measured with a standard precision of 0.25 percent the small quantity of CO_2 involved can be measured with a standard precision of 5.2 percent. Various parameters are being studied to improve these precisions.

6. Electron Microprobe Examination of Uranium-Plutonium Carbides
(E. A. Hakkila and H. L. Barker)

Approximately thirty samples of these materials from various experiments were examined to identify impurities, inclusions, and phases, and to determine homogeneity on a microscale. In most, the matrices were homogeneous with respect to U, Pu and C distributions, but some depletion of Pu and enrichment of U occurred in isolated areas in a few cases. Inclusions generally were enriched in Pu and depleted in U and C with respect to the surrounding matrix. Some contained Si, Fe, Cu, Ni, or W as impurities but not necessarily associated together. In two cases, a Pu-rich grain boundary phase was observed without detectable impurities. Needle-like precipitates were generally enriched in C.

7. Applications of Analytical Methods to the Analyses of Various Materials
(J. W. Dahlby, N. L. Koski, G. B. Nelson, M. E. Smith, L. E. Thorn, and W. W. Wilson)

Approximately forty-five samples of (U, Pu)C materials from various preparatory operations and experiments were analyzed for U, Pu, O, C, and N by controlled-potential, combustion, inert-gas-fusion, and Kjeldahl methods. Uranium concentrations varied from 74.6 to 78.7 percent, Pu from 16.8 to 19.9 percent, and C from 4.5 to 5.1 percent. Nitrogen generally was present at about 200 ppm but ranged from 105 to 485 ppm. Oxygen varied widely, depending on the history of the sample, from 25 to 1000 ppm. Eight samples of $(U, Pu)O_2$, having U/Pu atom ratios from 21/1 to 2.2/1 were analyzed for U and Pu by potentiometric titration with a precision < 0.1 percent. A few specimens of UC, PuN, and PuC were analyzed for major constituents.

V. REFERENCES

1. W. A. Lambertson and M. H. Mueller, J. Am. Ceram. Soc. 36, 366 (1953).
2. D. K. Smith and C. F. Cline, J. Am. Ceram, Soc. 15, 249 (1962).
3. W. L. Lyon and W. E. Baily, GEAP-4878 (1965).

4. W. H. Zachariasen, (1944) Manhattan Projects Repts. July. See also National Nuclear Energy Series (1949), 14B, 1449.

5. P. Costa and R. Lallement, Physics Letters, I, 21-22 (1963).

6. C. DeNovion, J. P. Krebs, P. Meriel, Comptes rendes. Acadimie des Sciences, 263B, 457-459 (1966).

7. A. E. Austin, Acta Cryst., 12, 159-161 (1959).

8. G. M. Campbell and J. A. Leary, J. Phys. Chem., 70, 2703 (1966).

9. J. A. Leary, R. L. Nance, W. C. Pritchard, J. C. Reavis, M. W. Shupe and A. E. Ogard, The Preparation and Properties of Plutonium Mononitride and Uranium Mononitride-Plutonium mononitride Solid Solutions, presented at the American Ceramics Soc. Symposium, Portland, Oregon, Oct., 1966.

10. J. B. Mann, J. Chem. Phys. 46, 1646 (1967).

11. W. M. Pardue, F. A. Rough and R. A. Smith, presented at AIME Nuclear Energy Symposium, Phoenix, Arizona, Oct., 1967.

12. M. H. Rand, Thermochemical Properties, in Atomic Energy Review, Vol. 4, Special Issue No. 1, IAEA, Vienna, 1966.

13. T. G. Godfrey, J. A. Wooley and J. M. Leitnaker, Oak Ridge National Laboratory Report ORNL-TM-1596 (1966).

14. R. C. Feber and C. C. Herrick, Los Alamos Scientific Laboratory Report LA-3184 (1965).

15. JANAF Thermochemical Tables, The Dow Chemical Co., Midland, Mich., 1964.

VI PUBLICATIONS

1. O. W. Djorklund, R. M. Douglass, and J. A. Leary, "Self-Irradiation Damage in Plutonium Ceramics" presented at Pacific Coast Regional Meeting of the Amer. Ceram. Soc., San Francisco, Nov. 2, 1967.

2. J. L. Green, G. P. Arnold, J. A. Leary, and N. G. Nereson, "Crystallography and Magnetic Ordering in Plutonium Carbides by Neutron Diffraction" presented at Pacific Coast Regional Meeting of the Amer. Ceram. Soc., San Francisco, Nov. 2, 1967.

3. J. A. Leary and K. W. R. Johnson, "Thermal Conductivity of Uranium-Plutonium Carbide Fuels", presented at the Nuclear Metallurgy Symposium on Plutonium Fuels Technology, Metallurgical Society of the A.I.M.E., (LA-DC-9059) Phoenix, October 4-6, 1967.

PROJECT 808

COMPATIBILITY OF SODIUM-BONDED (U,Pu)C AND (U,Pu)N FUELS WITH CLADDING MATERIALS

Person in Charge: D. B. Hall
Principal Investigators: R. H. Perkins
J. A. Leary

I. INTRODUCTION

The use of sodium for heat transfer between the fuel pellets and the cladding is desirable to lower the surface temperature of the pellets and to permit substantial tolerances in the dimensions of the pellets and the clads. The objectives of this program are to study and understand the interactions of (U,Pu)C and (U,Pu)N with sodium and potential cladding materials and, if necessary, to modify the properties of these components to achieve a satisfactory sodium-bonded fuel element for a LMFBR. Emphasis is to be placed on the studies of sodium-bonded carbides in Type 316 stainless steel.

During the assembly of equipment and the development of procedures, some of the initial effort has been devoted to two surveys of the literature. The reports deal with the (U,Pu)C fuel[1] and (U,Pu)N fuel,[2] respectively. The surveys have shown that the published work and the fuels themselves have several strengths and weaknesses. For example, the data on the carbide fuel invariably emphasize the difficulty in obtaining single-phase, stoichiometric monocarbide and several reports document the unsuitability of the hypostoichiometric form or that containing dicarbide. The nitride fuel is comparatively easy to prepare in a pure form that is compatible with stainless steel. Considerable remains to be done with both fuels with respect to compatibility in- and out-of-pile, and regarding the techniques of preparation, handling, metallography, analysis, etc.

Carburization of a stainless-steel clad via sodium has received some attention in this laboratory[3] and warrants further study in regard to the compatibility of (U,Pu)C. Although no nitride fuel pellets are available, there is an interest in detecting the tramp contaminant U_2N_3 and in estimating its effect on an important clad like stainless steel. In addition to integral tests of compatibility in- and out-of-pile, more specialized studies of the following nature should also be pursued:

1. The effects of venting fuel capsules to the sodium coolant.
2. The effects of high concentrations of fission products in sodium bonds on compatibility.
3. The stability of the sodium bond under various stresses.

II. CARBIDE FUEL COMPATIBILITY STUDIES
(F. B. Litton, L. A. Geoffrion, J. H. Bender)

A. General

The objectives of this program are to study the interactions among single-phase mixed uranium-plutonium carbide, a sodium bond, and potential cladding materials, i.e., to investigate the technology related to sodium-bonded fuel elements. There are two approaches to the experimental work. One approach is to determine the reactions occurring between $(U_{0.8}Pu_{0.2})C$ and potential cladding materials, using Type 316 stainless steel and a high-strength vanadium-base alloy (V-15Ti-7.5Cr) as the first and second choice of cladding material, respectively. A second concurrent set of experiments is to study the mechanism of carbon transport through sodium, the effect of impurities such as oxygen, and the carburizing potential of sodium in mutual contact with carbides and the preferred cladding materials.

Capsules containing sodium-bonded, single-phase (U,Pu)C will be tested in sodium loops at 750°C for

periods up to 10,000 h. Primary emphasis will be placed on fundamental reactions occurring between $(U_{0.8}Pu_{0.2})C$ and Type 316 stainless steel or vanadium alloy. High-purity, thoroughly characterized sodium will be used for the studies. Fuels of known composition will be supplied using methods developed by Ceramic Plutonium Fuel Materials (807) program at LASL. Most of the testing will be performed on stoichiometric (U,Pu)C fuel; hypo- and hyperstoichiometric, mixed carbides will also be studied to determine the effect of the M/C ratio of the fuel on carbon transport by the sodium bond. Carbides containing known and controlled amounts of oxygen and nitrogen will be tested to determine the effect of these additives on the sodium bond and on fuel-clad compatibility. The Pu/U ratio in most mixed fuels will be maintained at 0.2, but some experiments will be performed on stoichiometric and hyperstoichiometric UC to determine the effect of plutonium addition on the behavior of the carbide fuel.

B. Current Results

1. Mechanism of Carbon Transfer

Apparatus for studying the mechanism of carbon transfer in the carbide-sodium-container system is in the final stage of assembly. The containment for the sodium is shown in Fig. 1. In addition, the apparatus contains a titanium sublimation ion pump and a purification train for the helium cover gas.

Type 316 stainless steel capsules are being analyzed to determine carbon transfer and change in sodium analyses after tests for 1000 h at 650° and 750°C. The capsules contained five grams of sodium and either stoichiometric or hyperstoichiometric uranium carbide. Companion capsules are in test containing sodium and either hypostoichiometric, stoichiometric or hyperstoichiometric uranium-plutonium carbides.

2. Corrosion Study

The behavior of selected cladding material in sodium is being investigated as a function of temperature and sodium purity. A group of six specimens each of vanadium, vanadium-10% titanium, vanadium-20% titanium, vanadium-40% titanium, vanadium-15% titanium-7.5% chromium, Types 304L and 316L stainless steel, niobium-1% zirconium, niobium-10% tungsten, and zirconium were immersed in zirconium-gettered sodium at 650°C for 1000 h. Reference is made to report LA-3820-MS for specimen analysis.

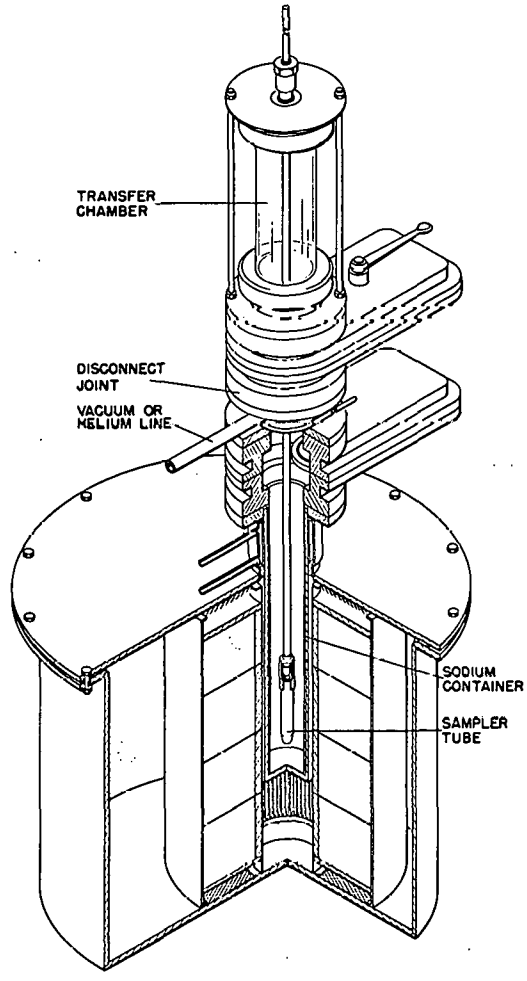

Fig. 1. Apparatus for studying carbon transfer in sodium.

The weight changes recorded in Table I indicate no significant corrosion of these materials in hot-trapped sodium at 650°C. For example, the weight loss of 0.048 mg/cm^2 on Type 304L stainless steel is approximately equivalent to a penetration of 2.6 microns per year. The films on the vanadium base alloys were insufficient for analysis. Average specimen weight changes at 650°C were about four times less than those recorded at 750°C.

3. Removal of Sodium Bond from Sintered (U,Pu)C Fuel Pellets

The purpose of this experimental program was to study the effect of various techniques for removing sodium from the fuel-to-clad sodium bond on

Table I

Corrosion of Materials in Hot-Trapped Sodium at 650°C for 1000 h

Material	Heat Treatment	Weight Change* (mg/cm^2)
V	Annealed 1 h, 900°C	+ 0.009
V-10Ti	Annealed 1 h, 900°C	+ 0.082
V-20Ti	Annealed 1 h, 900°C	+ 0.096
V-40Ti	Annealed 1 h, 900°C	+ 0.087
V-15Ti-7.5Cr	Annealed 1 h, 850°C	+ 0.183
Type 304L SS	Annealed 1 h, 1000°C	- 0.048
Type 316L SS	Annealed 1 h, 1000°C	none
Nb-1Zr	Annealed 1 h, 1350°C	none
Nb-10W	Annealed 1 h, 1350°C	- 0.046
Zr	Annealed 1 h, 850°C	+ 0.076

*Average of six one-half inch square specimens

the structure of single-phase, sintered, mixed-carbide fuel pellets. The techniques considered were distillation, dissolution in high-purity organic reactants, mercury amalgamation, and dissolution in liquid ammonia. The latter two techniques were held in abeyance until preliminary work was completed on distillation and dissolution techniques.

A purification loop served as the source of sodium for bonding (U,Pu)C fuel pellets to Type 316 stainless steel cladding material. The loop was operated at a bulk sodium temperature of 163°C (325°F) and a cold trap temperature of 130°C (265°F). The sodium was withdrawn from the loop in a glovebox containing less than 10 ppm of total impurities.

The sodium was then cast to form an extrusion billet. The billet was extruded into 0.240-in.-diam rods, which were cut to 1-in. lengths. Capsules of Type 316 stainless steel (0.30-in. o.d. by 0.10-in. wall by 3 in. long) were loaded with three mixed-carbide fuel pellets (0.265-in. diam by 0.25-in. long) and one length of extruded sodium. After the closure welds were made, the capsules were removed from the dry box, heated to 600°C (1112°F) for 1 h and centrifuged while cooling to room temperature. They were reheated to 300°C (572°F) and placed in a magnetostrictive device for 1 h. The integrity of the bond was inspected by x-ray, ultrasonic, and eddy-current techniques.

In the dissolution techniques, the sodium bond was removed from the fuel pellets by reaction with pure butyl and ethyl alcohols, and with ethyl alcohol containing 5 vol.% of distilled water. It was conducted in an open hood, which was periodically checked for alpha contamination during the processing.

The capsules were cut with a tube cutter approximately 1/4 in. above the sodium level. The opened capsules were then immersed in a beaker in the respective reactants until the top fuel pellet was exposed. The clad was cut from around the top pellet exposing the sodium bond. The capsule was then immersed in the reactant until there was a noticeable decrease in hydrogen evolution. This procedure was repeated until the exposed pellet could be removed from the clad. When evolution of hydrogen ceased, the fuel pellets were removed from the reactant, dried by swabbing with cheese cloth, and stored under vacuum prior to metallography.

The removal of the sodium bond by reaction with alcohols proved to be a time-consuming operation. The pellets were removed in 3-1/2, 5-1/4, and 7 hours with ethyl alcohol containing 5 vol.% of water, absolute ethyl alcohol and pure butyl alcohol, respectively. No serious problem was encountered as a result of alpha contamination. As anticipated, counts were observed on tools used for decladding, but otherwise alpha contamination was restricted to particulate matter mechanically detached from the exposed pellets.

In the distillation technique, the sodium bond was removed from the fuel pellets by distilling the sodium under vacuum at a relatively low temperature. A vacuum of 5×10^{-6} torr and a temperature of 475°C (887°F) was adequate to free the pellets of sodium. A schematic view of the distillation unit is shown in Fig. 2.

The capsules were opened in an open hood by cutting with a tube cutter approximately 1/4 in. above the sodium level. They were placed in the capsule block and transferred to the distillation unit. The distillation unit was sealed and a vacuum of 5×10^{-6} torr attained. The furnace was then heated to 485° $\pm$ 10°C, and the temperature maintained there until the vacuum was re-established in the 10^{-6} torr range. This required a period of six hours. The furnace was cooled overnight to room temperature.

The distillation unit was then opened. The cold finger was removed and the condensed sodium was reacted with ethyl alcohol. The block containing the capsule was removed from the distillation unit.

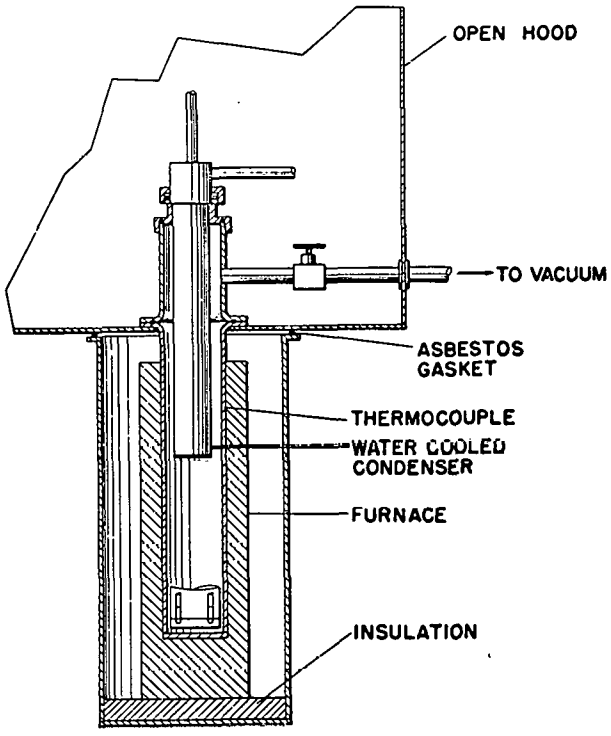

Fig. 2. Schematic view of the sodium distillation unit.

After end-flaring the capsule for pellet removal, the pellets were removed and packaged for transfer to metallography. The open hood, tools, and all parts to the distillation unit were then monitored for alpha contamination. As a general rule, there was no contamination problem except for those tools or parts which had been in direct contact with the pellets.

All (U,Pu)C fuel pellets were sectioned longitudinally and vacuum-impregnation mounted in epoxy resin. The mounted sections were ground on SiC papers through 600 grit using lapping oil as the lubricant. Polishing was performed by hand and with automatic equipment on synthetic napless lap coverings using 15 μ, 6 μ, and 1 μ diamond paste with silicone oil as the lubricant. The samples were ultrasonically cleaned with vythene between each preparative step. The specimens were then electrolytically etched with 1:1:1 lactic, nitric, and acetic acids (2.5 V dc, 9 sec, touch probe). This polishing and etching sequence was then repeated prior to photomicrography.

The grinding and polishing lubricants were analyzed for their water content. Lapping oil contained 0.04 w/o water, while silicone oil and vythene contained 0.03 and 0.02 w/o of water, respectively. Extended exposure of these lubricants to a washed-air environment showed no measurable absorption of moisture from the atmosphere. Molecular sieves were placed in the lubricant containers to absorb the small percentage of water prior to use.

The structure of sintered (U,Pu)C was studied by metallography after removing the sodium bond by dissolution and distillation. Porosity was determined by the method of two-dimensional, systematic, point count. The porosity after sodium removal was compared to unbonded "as-received" pellets. The data on porosity were obtained from at least three pellets for each technique and are presented in table II.

Table II

Effect of Sodium Removal Techniques on the Porosity of (U,Pu)C Pellets

Technique	Average Porosity (%)	Maximum Porosity (%)	Maximum Pore Size (μ)
Unbonded	10.1	11.0	16.6
Ethanol	12.5	13.0	21.8
Butanol	11.7	12.2	16.2
Distillation	8.5	10.0	12.9
Ethanol + 5% H_2O	19.7	23.3	33.3

The data show that the low-temperature vacuum distillation is the preferred method for removing sodium from sodium-bonded fuel capsules. Sodium distillation has no appreciable effect on either the size or shape of the pores. However, both the size and shape are changed by dissolution techniques. Butanol has less effect on the microstructure than ethanol. Dissolution techniques (ethanol and butanol) produce a rounding of the pore edges, probably because the dissolution did not effectively remove all of the sodium prior to metallography. However, the vacuum-distillation technique retains the original sharp pore edges while removing all of the sodium. These conclusions are supported by structures shown in Fig. 3 through 7.

Figure 3 is typical of the pore size and shape of a single-phase (U,Pu)C pellet not exposed to sodium. The pore edges were sharp and distinct.

Figure 4 is an example of the effect of the ethanol dissolution of the sodium bond. Apparent porosity had increased and many of the pore edges

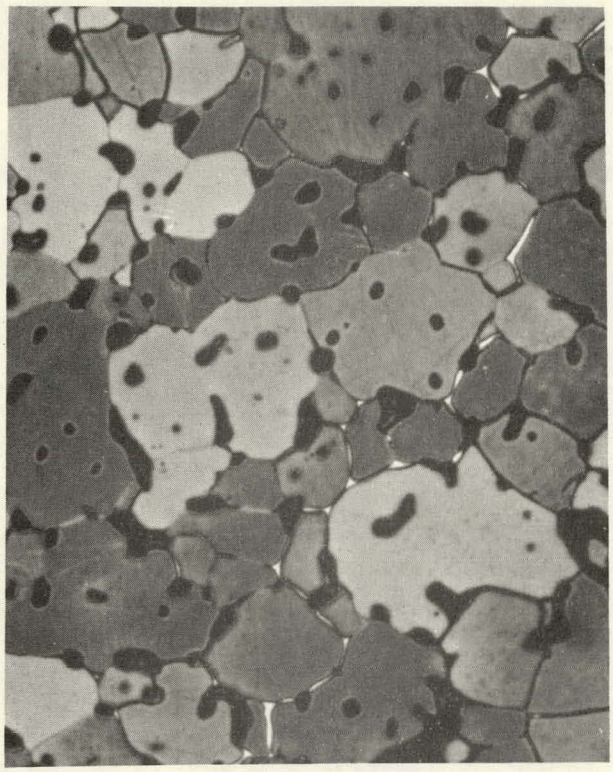

Fig. 3. (U,Pu)C, etched, 300X. Unbonded reference sample.

Fig. 5. (U,Pu)C, etched, 300X. Butanol dissolution of sodium bond.

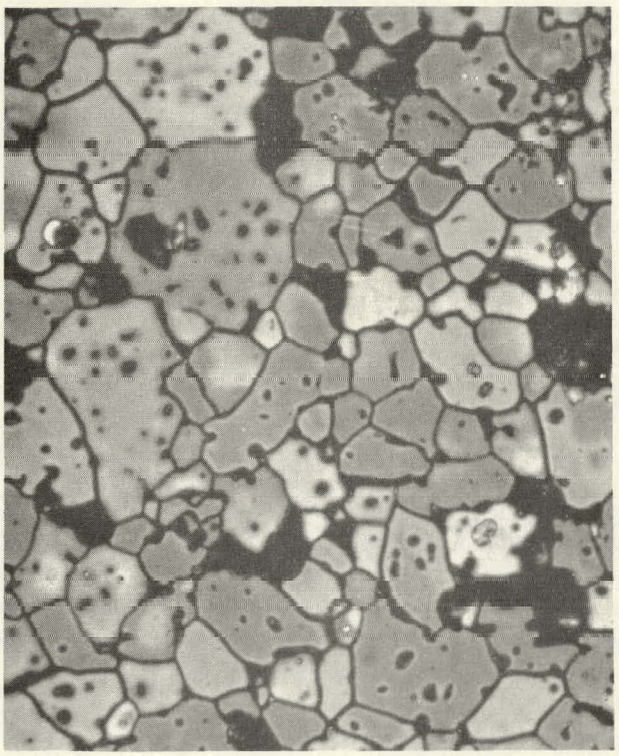

Fig. 4. (U,Pu)C, etched, 300X. Ethanol dissolution of sodium bond.

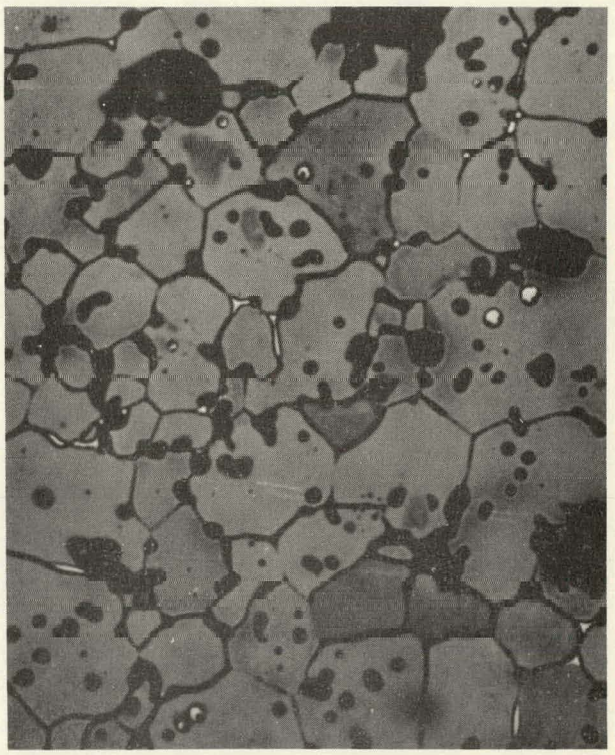

Fig. 6. (U,Pu)C, etched, 300X. Vacuum distillation of the sodium bond.

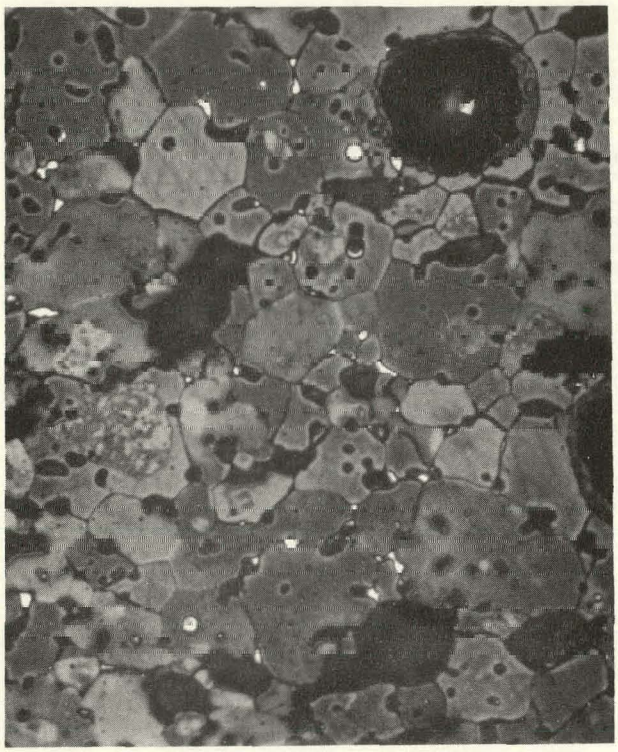

Fig. 7. (U,Pu)C, etched, 300X. Ethanol-5% water dissolution of sodium bond.

were rounded. Small amounts of sodium continued to seep out of the sample during metallography.

Figure 5 shows the typical result of a butanol dissolution of the sodium bond. The over-all changes in porosity and pore shape were not as severe as they were following the reaction with ethanol, but substantial amounts of sodium reaction products continued to seep out of the specimen.

Figure 6 illustrates the effect of the removal of the sodium bond by vacuum distillation. Pore measurements indicate no deleterious effects; the pore edges retained their original sharp edges and seepage of sodium reaction products was not observed.

Figure 7 shows the severity of attack to the pores caused by the addition of 5 vol.% of water to the ethanol. Over-all porosity appeared to double; pore shape was no longer well defined and sodium continued to give seepage reaction products. (Evidence for the latter are ring-shaped stains and a general "blotchy" appearance).

III. VENTED (U,Pu)C EXPERIMENTS
(J. C. Clifford)

A. General

Sodium and single-phase (U,Pu)C are being contacted in a small forced-convection sodium system for periods of 1000 h and longer. The experiments are limited to determining the out-of-pile stability of single-phase (U,Pu)C in flowing sodium in support of studies of fission product release from the same material during and after neutron irradiation.

The sodium loop used for these experiments consists of three inter-connected vertical legs and a dump tank (Fig. 8). Two legs contain fuel test sections, and the third contains a replaceable zirconium hot trap and an immersion heater. All sodium-wet sections of the loop are Type 316 or 321 stainless steel and the nominal operating temperature of

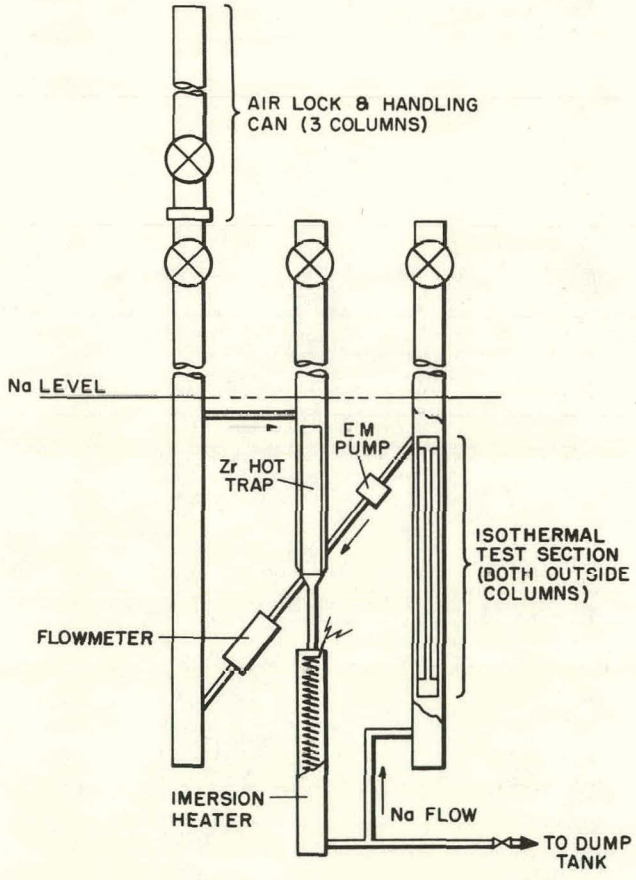

Fig. 8. Schematic of 700°C isothermal sodium system for (U,Pu)C venting experiments.

the system is 700°C. The sodium capacity of the loop is < 10 lb, and the mass flow rate is 300-400 lb/h, providing a velocity on the order of an inch per second in the fuel test sections.

Pellets of approximately 92% dense mixed carbide (0.265-in. diam, 0.25-in. long) are inserted in tubes of Type 316 stainless steel (0.300-in. o.d., 0.010-in. wall), three pellets per tube. The fuel occupies approximately 3/4 in. of the 3-in.-long tubes. In some cases the tubes are open at both ends to allow sodium flow between fuel and tube; in others the tube is closed at the bottom to maintain a static sodium bond between fuel and tube during test.

Typical sodium impurity levels in the system are < 5 ppm O, < 4 ppm N, and < 5 ppm H. Sodium samples can be obtained for determination of U, Pu, and total C.

B. Current Results

The first set of three capsules, two flow-through and one static, was removed from test after 900 h at 700°C. Sodium was removed from the capsules by dissolution with "absolute" ethanol and the pellets and cylinders were examined metallographically and by electron beam microprobe. Aside from an increase in pore size, attributable to the use of water-contaminated ethanol for removal of sodium, and some cracking along the ends, the pellets appeared unchanged after test (Fig. 9). Microprobe traverses from edge to center of the pellets failed to detect any variations in pellet composition. The stainless steel cylinders also appeared unchanged after test (Fig. 10), and microprobe traverses of the walls did not detect the presence of U, or any C, Fe, Cr, or Ni gradients. Alpha contamination of these tubes and stainless steel brackets in the system was generally < 5000 d/m-in.^{2}

A duplicate set of capsules has been removed for examination after 2000 h of exposure.

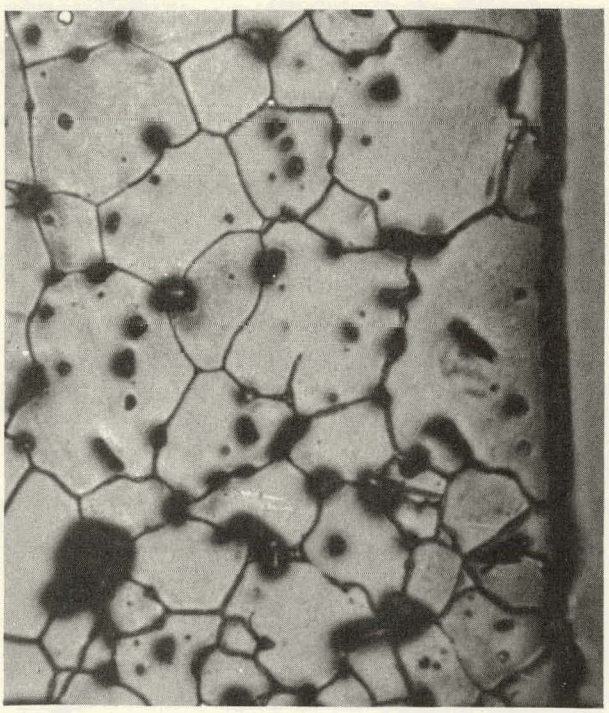

Fig. 9. Surface region of a (U,Pu)C fuel pellet after 900 h in 700°C sodium. 300X

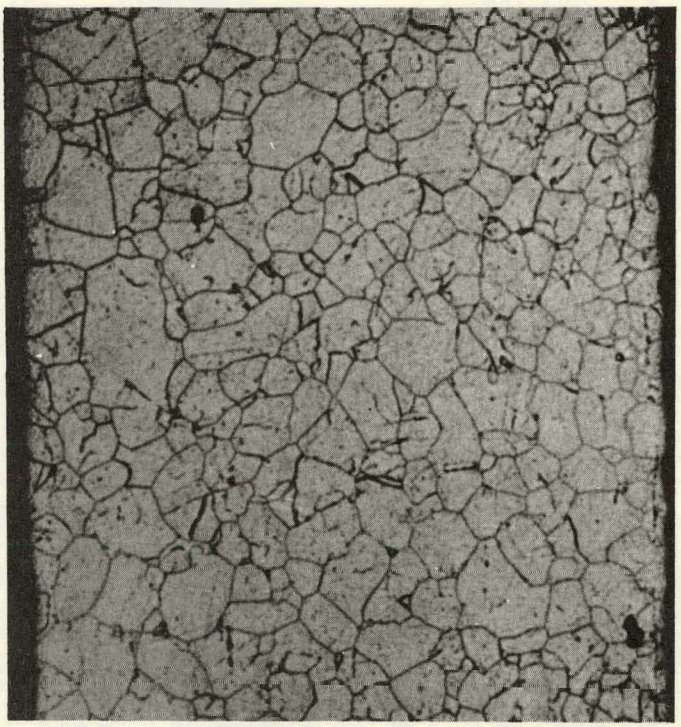

Fig. 10. Section of Type 316 stainless steel tubing from a vented (U,Pu)C fuel capsule after 900 h in 700°C sodium. 300X

IV NITRIDE FUEL STUDIES
(B. J. Thamer)

A. General

Although not the most studied of ceramic fuels, (U,Pu)N is nevertheless one of the most promising because of its ease of fabrication, compatibility with inexpensive clads, resistance to radiation, etc.[2] In spite of the fact that fuel pellets have been unavailable, some attention has been given to the probable effect of the contaminant U_2N_3 as it might affect the favored clad, stainless steel.

B. Current Results

The availability in the literature of data on the absorption of nitrogen from NH_3 or N_2 by Type 304

stainless steel has prompted some estimates of whether U_2N_3 would produce a nitride precipitate in this steel. The data suggest that such precipitation could take place somewhat below 400°C but the process would probably be slow at such low temperatures. The data above the region of sensitization for this steel were too inconsistent of reliable estimates.

V. LOADING FACILITY FOR TEST CAPSULES
(D. N. Dunning)

A. General

A prerequisite to a compatibility program involving (U,Pu)C, sodium, and potential cladding materials is a satisfactory capsule loading and bonding facility. There is little point to obtaining well-characterized materials for testing if these materials are contaminated before they are placed in test. Sodium and (U,Pu)C are sufficiently reactive that all operations must be performed either in vacuum or in a high-quality inert atmosphere. A loading facility for handling these materials is now operational; however, it is far from being complete. An inert-atmosphere glovebox for handling fuel pellets prior to their insertion into capsules must still be installed. In addition, inert gas cleanup systems must be incorporated into the facility.

B. Current Results

1. Fuel Loading Station

A new two-section, evacuable, inert-atmosphere glovebox for fuel pellet loading and inspection has been received at LASL. Piping and installation have been initiated. This box will have one section that will be used for inspection of fuel pellets and will be "alpha hot." The other section of the box will be maintained in the "alpha cold" condition. Fuel pellets will be loaded into capsules through the box wall separating the two sections. Inert gas purity will be maintained in both sections of the box.

The present fuel pellet loading is accomplished in the sodium loading box to ensure that the fuel pellets do not see any air during loading operations. Forty-five capsules of various configurations were loaded during the past quarter. The pellets are laid on aluminum foil during loading; this foil is then disposed of to control alpha contamination in the sodium loading box, since this box is maintained in the "alpha cold" condition.

Two of the capsules are for irradiation tests in the Omega West Reactor (OWR). The loading techniques used on these capsules were the same as those proposed for use on the 3-ft-long EBR-II irradiation test capsules.

2. Sodium Purification Loop and Sodium Loading Box

The sodium purification loop and loading box are operational on a routine basis.

3. Sodium Bonding

Eighteen capsules were bonded during this quarter using the following procedure:

a. Heat the loaded and welded capsule to 600°C for 1 h with sodium on bottom.
b. Centrifuge until the sodium is frozen.
c. Reheat the capsule to 300°C for 1 h with magnetostrictive device operating against the capsule bottom.
d. Centrifuge until the sodium is frozen.

In addition, two irradiation capsules were bonded using a modified procedure which is proposed for long capsules for which centrifuging is impractical. The fuel pellets are positioned on the capsule bottom by melting the sodium and forcing the pellets into the liquid sodium with a spring. The sodium is then frozen and the final closure weld is made. The heating cycles for sodium bonding are the same as those in the standard bonding procedure; however, the centrifuging step is omitted.

VI. POST-TEST EXAMINATION
(J. H. Bender)

A. General

Metallographic examination is one of the primary methods for evaluating the compatibility of fuels with cladding; however, delineation of the phases that may be present in sintered (U,Pu)C (metallic, dicarbide and sesquicarbide) has been inaccurate with all of the known metallographic techniques. Continued investigation of multiple techniques has succeeded in developing a stain etch, microhardness and preferential etch method that accurately distinguishes between the metallic, dicarbide and sesquicarbide phases of (U,Pu)C and precipitates of PuSi.

B. Current Results

Differentiation of the metallic, dicarbide, and sesquicarbide phases by optical means, i.e., grain shape and precipitate shape, has proved effect-

ive only with the dicarbide phase that appears as needle-shaped precipitates within the grains. When other precipitates occur in conjunction with the dicarbide phase, it is safe to assume they are sesquicarbide precipitates.

Preferential etches to remove metallic precipitates[4] have proved effective on 65% of the samples tested. The unreliability of this technique is attributed to the metallic particles having a retained oxide film that prevents dissolution by the etchant.

Diamond point microhardness testing of precipitates and the surrounding matrix has proved effective in detecting the metallic phase, since the metallic phase has lower hardness than the matrix. However, precipitates with higher hardness numbers have been reported by electron beam microprobe examination as, PuSi, sesquicarbides, or areas of higher-than-average density.

Continued investigation of the microhardness technique and other preferential etches revealed the following information:

a. The crystal faces of matrix grains in polished and normal stain-etched specimens vary in hardness as color varies; i.e., the faces that etch darker are an average of 150 numbers in hardness lower than the crystal faces that etch light in color.

b. The plutonium silicides range from 100 to 300 numbers higher in hardness than the matrix and are comparable in hardness to sesquicarbides.

c. A preferential etch for PuSi (HF-HNO_3-methanol, 1:1:3)[5] applied after the usual electro-etch (HNO_3-HAc, lactic, 1:1:1) produces a green, red, or orange coloration of the PuSi precipitates, removes all of the coloration of the matrix grains and does not affect the white coloration of metallic or sesquicarbide precipitates.

From these observations, the following procedure was developed which permits fast metallographic analysis:

a. Sample of unknown stoichiometry is etched with the usual electrolyte to distinguish grain boundaries and white precipitates as shown in Figs. 11 and 12.

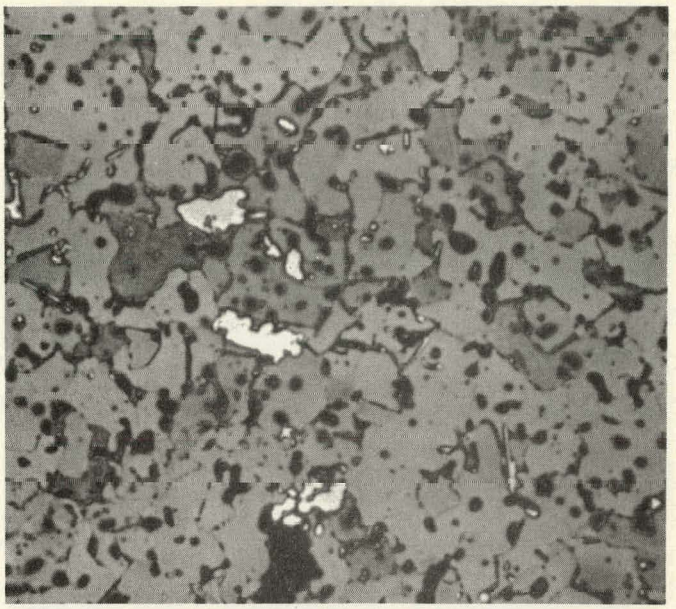

Fig. 11. Hypostoichiometric (U,Pu)C. Electro-etched, 400X. Grains and precipitates evident, microhardness (DPH 25 g and 100 g wts) of matrix 780 to 900, precipitates 695 and 1100.

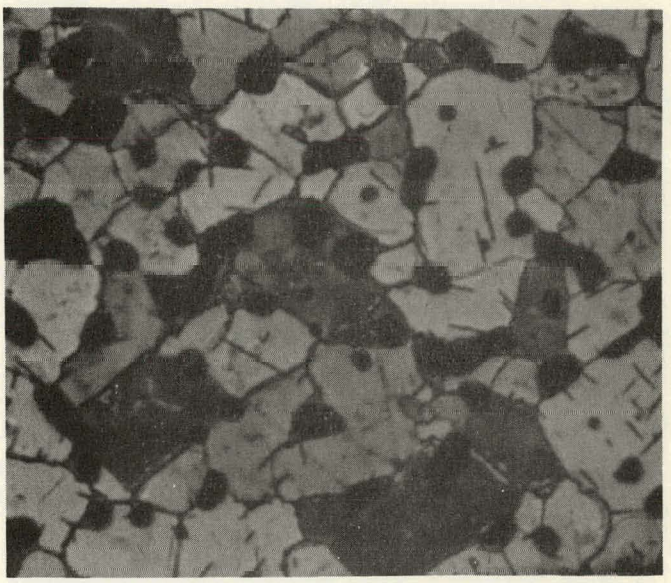

Fig. 12. Hyperstoichiometric (U,Pu)C. Electro-etched, 400X. Grains, dicarbide needles, and precipitates evident. Microhardness of matrix 950 to 1095, precipitates 1200.

b. Precipitates are microhardness tested to determine if metallic phase is present or if the precipitates are harder than the matrix.

c. When harder phases are present, sample is re-etched with the PuSi preferential etch, as shown in Fig. 13.

d. If precipitates develop a color, PuSi is present, and if they are colorless, the precip-

itates are sesquicarbide. A typical example is shown in Fig. 14.

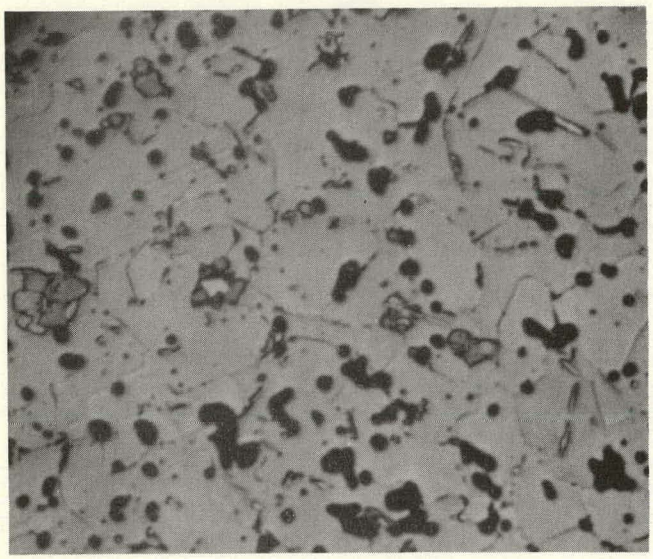

Fig. 13. Hypostoichiometric (U,Pu)C. Preferential etch for PuSi, 400X. Agglomerates of metallic and PuSi precipitates. M = white PuSi = dark precipitates.

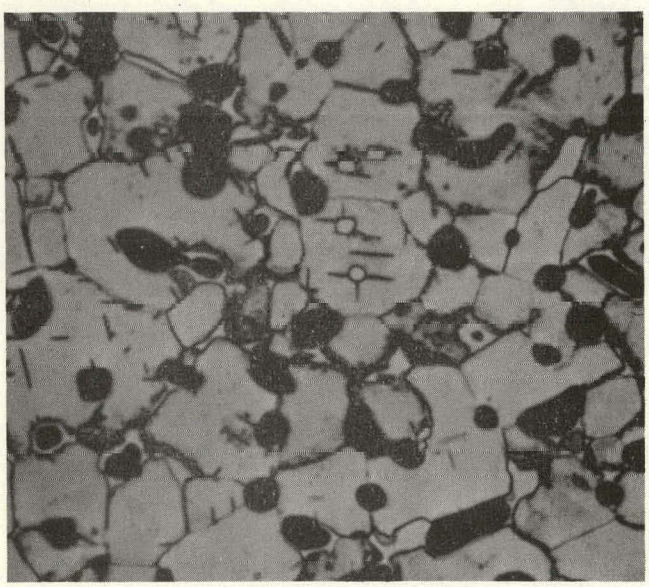

Fig. 14. Hyperstoichiometric (U,Pu)C. Preferential etch for PuSi, 400X. Agglomerates of M_2C_3 and PuSi precipitates. M_2C_3 = white, PuSi = dark precipitates. Note growth pattern of M_2C_3, which is angular when developing between dicarbide platelets and less angular when developing at intersections of MC_2 platelets.

VII. EBR-II IRRADIATION TESTING
(J. O. Barner)

A. General

The purpose of these irradiations is to evaluate candidate fuel/sodium/clad systems for the LMFBR program. In the reference design, pellets of single-phase (U,Pu)C are separated by a sodium bond from a cladding of Type 316 stainless steel or other high-temperature alloy. Seven fuel-element tests are planned in the initial group of a continuing series of irradiation experiments.

The capsules are to be irradiated under the following conditions:

1. Lineal power: 29.15 to 30.20 kW/ft (max).
2. Fuel composition: $(U_{0.8}Pu_{0.2})C$, (single-phase, sintered, fully enriched).
3. Fuel density: 85% and 90% of theoretical.
4. Smear density: 75% and 80%.
5. Clad size: 0.300 in. o.d. x 0.010 in. wall.
6. Fuel size: 0.265 in. diam x 0.25 in. high.
7. Clad type: 316 SS and Hastelloy-X.
8. Maximum clad temperature: 1250°F.
9. Maximum fuel centerline temperature: 2130°F.
10. Burnup: 0.22 to 0.66 g fissioned per cm^3.

B. Current Results

The hazards report (LA-3768-MS) for the irradiations has been issued.

Parts have been completed for mockups necessary to test bonding procedures.

VIII. THERMAL FLUX IRRADIATIONS
(J. O. Barner, R. L. Cubitt, D. C. Kirkpatrick)

A. General

Two environmental cells had been installed in the Omega West Reactor (OWR) for the irradiation of liquid plutonium-alloy fuels. With little modification, they will be suitable for test irradiations of (U,Pu)C fuel elements.

An EBR-II mockup capsule has been designed for insertion in one of these cells in the OWR. This capsule is a shortened version of those designed for EBR-II and is intended to test the end closures and hold-down devices as well as to evaluate the high heat flux, sodium-bonded region of the capsule.

B. Current Results

One environmental cell and its associated instrumentation and gas system were checked out to

prepare for irradiation of a capsule containing (U, Pu)C fuel pellets. In order to investigate the cell performance, an unfueled insert was installed in the cell and operated with electrical heat. Heat balance measurements agreed with those obtained when the cell was first installed in the reactor, demonstrating proper cell operation. Measurements made with helium only in the heat leak gas annulus indicate that appropriate temperature ranges can be maintained for the fuel capsule.

When the insert was withdrawn from the cell, some activity was observed in deposits on the insert. One deposit was apparently sodium, and the other was black and not immediately identifiable. Scrapings were taken from the deposits and were gamma scanned. The main sources of gamma activity were found to be ^{22}Na, ^{54}Mn, and ^{182}Ta from the reactions $^{23}Na(n,2n)^{22}Na$, $^{54}Fe(n,p)^{54}Mn$, and $^{181}Ta(n,\gamma)^{182}Ta$. Smaller sources were also found, but have not yet been identified.

Although the environmental cell has not operated for nearly a year, only small difficulties were encountered, most of them due to instrumentation.

On December 18, 1967, Environmental Cell #1 was removed from the reactor. This cell was installed in the reactor during April 1965 and was in operation until October 1966. For the past year, it was not operated and remained withdrawn from the core region. The removal proceeded without difficulty; the maximum dose received by personnel was 0.04 R. The cell will be gamma scanned and radiographed, and then disassembled for visual and metallographic examination.

Two EBR-II mockup capsules have been loaded and are being bonded and nondestructively tested. The best of the two will be selected for loading in the test cell. The capsule will operate at 35.9 kW/ft for one week in the OWR.

IX. SODIUM-BOND HEAT-TRANSFER STUDIES (J. O. Barner)

A. General

The purpose of this project is to evaluate methods for determining the effects of fuel-pin defects on heat-transfer properties of the sodium bond. Such defects could arise in a number of ways. For example, a void in the sodium bond could (1) be present before insertion in the reactor, (2) come from de-wetting of the pellet due to change in composition as fission products are formed, (3) form from a hot spot on the pellet and consequent local vaporization of the sodium, and/or (4) be produced from desorbed or fission-product gases. Of these, probably the most serious defect would be the presence of fission-gas bubbles in the bond region.

There appear to be three methods of obtaining the high heat fluxes necessary for "defect analysis": (1) in-pile experiments, (2) out-of-pile experiments utilizing a central, high-heat-flux heater, (3) out-of-pile experiments utilizing an induction heat source with the heat flow direction reversed. These three methods are all receiving consideration for use in sodium-bond heat-transfer studies.

B. Current Results

In an effort to develop instrumentation which will indicate the magnitude of defect effects, the size and shape of bubbles in appropriate geometric systems are being investigated. Water-plexiglass-air and water-glass-air combinations were used for the initial tests to determine the behavior of bubbles. The test geometry for both cases utilized flat plates with variable gaps. The gap was varied from 0.0042 in. to 0.0105 in. Bubbles were inserted with a hypodermic needle. Initial experiments utilized plates washed with a mild soap and rinsed in distilled water. The following qualitative results were observed.

1. Water-Plexiglass-Air, 0.0105-in. Gap

   Bubbles initially inserted were approximately circular. After some period of time (1 to 5 min), the bubble began to become unstable and a "finger" began to form on the upper surface of the bubble which continually grew at the expense of the bulk of the bubble until length-to-width ratios of approximately 5 to 1 were obtained. At this point (1 to 10 min after formation of the bubbles), the whole bubble began to move upward at a velocity of about 2.25 cm/min. Bubble sizes were about 4 to 5 x 10^{-2} cm^3. Larger bubbles took less time to start moving and attained slightly higher velocities.

2. Water-Plexiglass-Air, 0.0065-in. Gap

   The behavior was essentially the same for this width of gap as for the 0.0105-in. gap,

except that bubble surfaces were much more irregular and the bubbles did not reach a terminal velocity after having traversed 10 to 15 cm. A bubble with a volume of approximately 5×10^{-2} cm^3 did not move, while bubbles with volumes of 8×10^{-2} cm^3 did move.

3. Water-Plexiglass-Air, 0.0042-in. Gap

Bubbles produced in this gap often had very asymmetric geometries and often left large remnants behind once they started to move. In general, the bubbles were difficult to produce and to evaluate. Long periods of time (2 to 4 h) were required to produce a bubble close to the critical size for movement and to wait for it to become unstable. Bubbles normally moved along exactly the same path that previous bubbles had taken. Remnants of the same size, shape, and location were normally left behind. Obviously, particular areas upon one or both of the plates had different surface characteristics than the bulk of the areas on the two plates. These areas of changing surface tension allowed bubbles to move either easier or harder than along the rest of the plate.

4. Water-Glass-Air, 0.0062-in. Gap

Bubbles in this system behaved similarly to bubbles in the plexiglass system. After initial "finger" formation, the bubble moved upward. However, terminal velocities in the range 5 to 30 cm/min were easily reached. For moving bubbles, length to width ratios of approximately 5 to 13 were typical. Moving bubbles left many remnants behind and normal bubble paths were from remnants to remnant, thus assisting movement in the upward direction. Bubbles with length-to-width ratios of greater than 4.5 and volumes of greater than 3.5×10^{-2} cm^3 easily moved, while bubbles with smaller volumes did not form the "finger" and hence did not move.

5. Water-Glass-Air, 0.0042-in. Gap

Bubbles in this system behaved similarly to the water-glass-air, 0.0062-in.-gap case. Large asymmetric bubbles were formed which left many large remnants behind as they moved.

The above experiments revealed that the movement, shape, and size of bubbles are dependent upon surface inequalities from area to area on the plates. Therefore, the glass plates were cleaned with a sulfate acid/potassium dichromate cleaning solution in an effort to obtain clean surfaces. The following results were observed:

6. Water-Glass-Air, 0.0042-in. Gap

Bubbles were easily formed. They moved readily and maintained a smooth shape which resembled an inverted pearshape. Typical length-to-width ratios were 1.5. No finger formation was necessary or observed to initiate movement. Typical velocities were from 50 to 200 cm/min, depending upon size. Bubbles as small as 0.40×10^{-2} cm^3 moved. No remnants were left behind as the bubble moved.

Obviously, the surface condition determines the way in which bubbles are formed and move. It is probable that bubbes in a sodium-bonded fuel element will behave more like the "dirty" surface types of bubbles in the water-glass-air system due to variable gaps and irregular surfaces.

A computer calculation was made to estimate the temperature distribution on cladding surfaces adjacent to bubbles in the sodium bond, under the conditions to be expected in large LMFBR systems. Figures 15, 16, and 17 illustrate the geometry used

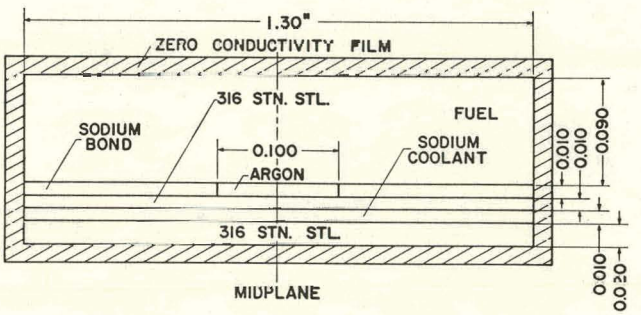

Fig. 15. Calculation model for bubble in sodium bond problem.

in the calculation and the results at heat fluxes of 1×10^6 and 2×10^5 Btu/h-ft^2. The temperature increases adjacent to the bubble appear to be measurable for the 1×10^6 Btu/h-ft^2 case. Inclusion of radiative heat transfer, which is ignored in this calculation, would decrease the depth of the temperature "well" in the clad surface temperature. Further calculations are being made to determine the error that can be expected due to heat losses from

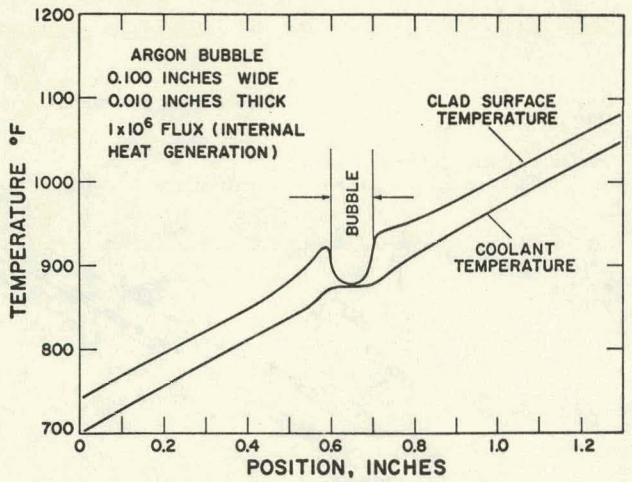

Fig. 16. Temperature perturbation caused by bubble in sodium bond (10^6 Btu/h-ft^2).

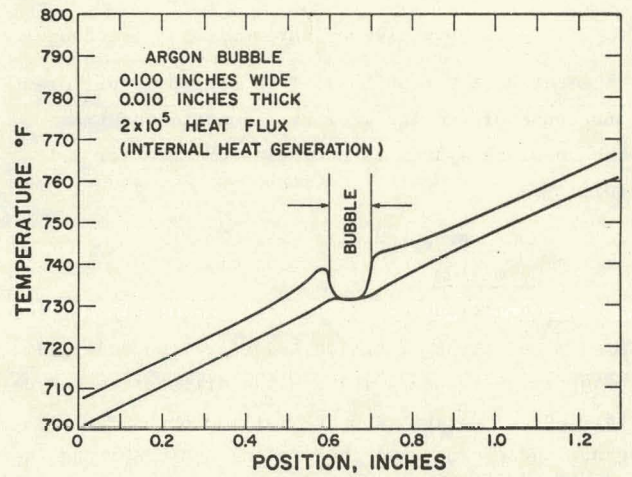

Fig. 17. Temperature perturbation caused by bubble in sodium bond (2×10^5 Btu/h-ft^2).

thermocouples used to measure the clad surface temperatures (see Thermal Scanner following).

Thermal Scanner

The feasibility of scanning clad temperatures with small sheathed thermocouples is being investigated. If sufficiently fine resolution can be achieved, the size and location of bubbles in bond sodium can be sensed by temperature measurement on the coolant side of the clad (see Figs. 16 and 17).

The scanner consists of a series of thermocouples mounted in a rotating rod in the center of flowing coolant and arranged to lightly contact the clad of an "inverted" fuel element; i.e., clad annular fuel being cooled by flow through the center of the element. A crude mockup of the concept, electrically heated and cooled by air, gave promising results. The assembly was rotated by a lathe and temperature differences of 3°C caused by heat loss to the lathe chuck jaws could be detected.

A prototype scanner for operation in flowing sodium and employing induction of the UC fuel is being designed.

X. GAMMA SCANNING AND OTHER STUDIES

(D. M. Holm, J. L. Parker, W. M. Sanders, B. M. Moore, H. M. Ruess, W. L. Briscoe)

A. General

Work on improved gamma-scanning techniques continues, and equipment to measure short-lived fission-product yields from fast-neutron-induced fission in plutonium is being constructed. The ^{3}He activation technique for the determination of oxygen and carbon in germanium and carburized stainless steel is also being investigated.

B. Current Results

1. Gamma Scanning of Short-Lived Fission Products from Fast Fission of Plutonium

An automatic system has been constructed to transfer plutonium samples for irradiation and counting. The electrical relay circuitry for the sample changer is shown in Fig. 18, the main assembly is shown in Fig. 19, and a cutaway view is shown in Fig. 20. The relay logics allow three modes of operation: automatic, one-cycle, and manual. In the automatic mode, depressing the start button causes a sample to be pneumatically transferred from the storage chamber into the irradiation station, where it is irradiated for a predetermined length of time. When the irradiation period has ended, the sample is blown back to the detection station, and a signal is sent to the analyzing equipment to start counting. Upon termination of the counting period, the analyzing equipment signals the automatic sample changer logics to proceed. The sample is then returned to the storage chamber, and the next sample is blown toward the irradiation station.

In the one-cycle mode, the operations are also sequenced automatically; however, at the end of a cycle, the system waits for the operator to signal for the start of the next cycle. In the manual mode, the operator initiates all the operations manually with push buttons.

This sample transfer system has been connected to a 4096-channel analyzer. As the gamma radiation

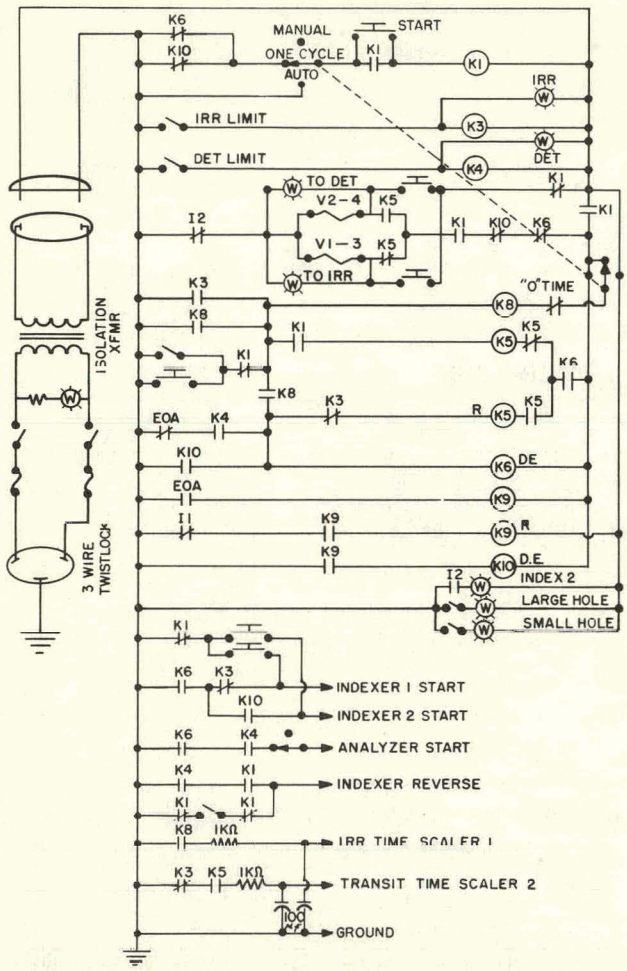

Fig. 18. Electrical relay circuitry for automatic sampler changer (standard JIC sysmbols).

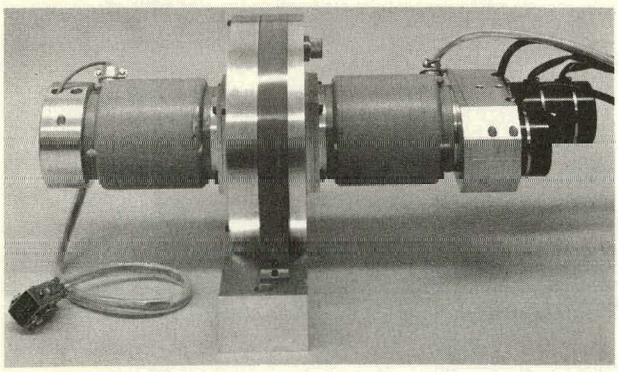

Fig. 19. Main assembly of automatic sample changer.

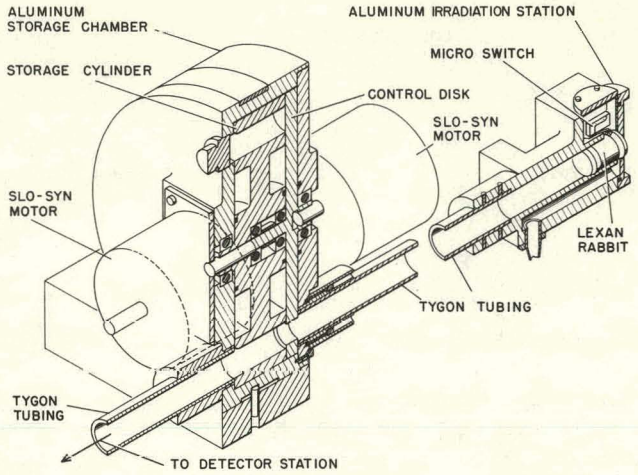

Fig. 20. Cutaway view of automatic sample changer.

is counted, the results will be stored in different subgroups of the analyzer as a function of time. The complete system is now being checked for reliability.

2. ^{3}He Activation

Germanium

Channeling of ^{3}He ions in single-crystal germanium and its application to activation analysis is being investigated. The crystal orientation was determined by directing a beam of low angular divergence and energy onto the crystal and observing the decrease in counting rate from Rutherford backscattered particles as a function of incident beam angle. Some samples were activated with the beam aligned along the [111] axis of the crystal and others with the beam purposely misaligned from that axis. Samples of germanium from different sources were analyzed, and typical values of 10 ppm oxygen and 40 ppm carbon were obtained. Slight activation of the germanium was found at 6.5 MeV and serious activation at 8 and 12 MeV. Autoradiography was performed on some of the samples following activation to aid in the interpretation of the results. Results are given in Table III.

Carburized Stainless Steel

An experiment has been performed which shows that ^{3}He activation in conjunction with autoradiography will give good measurements of both the concentration and the concentration gradient of carbon

Table III

Results of ^{3}He Activation Analysis on Germanium

Sample	Date	Energy* (MeV)	Total Charge (coulomb)	Irradiation (min)	Concentration Carbon† (ppm)	Concentration Oxygen† (ppm)	Ratio C/O
B-3	8/ 4/67	7.0	5.42×10^{-4}	50.0	85	21.0	4.0
D-4	8/ 9/67	6.5	2.26×10^{-3}	87.0	74	19.0	3.9
J-1	8/15/67	6.5	1.49×10^{-3}	90.0	70	12.0	5.8
T-7-B	8/15/67	6.5	1.42×10^{-3}	90.0	63	13.0	4.8
4-S	8/15/67	6.5	1.39×10^{-3}	90.0	53	12.0	4.4
NBS-53	8/17/67	6.5	1.51×10^{-3}	90.5	40	0.97	41.0
NBS-39-1	8/17/67	6.5	1.93×10^{-3}	122.0	55	0.50	100.0
D-8	8/31/67	8.0	1.01×10^{-4}	64.5	36	14.0	2.6
D-11††	8/31/67	8.0	1.56×10^{-4}	60.8	80	13.0	6.3

*All samples were etched to depth of 0.55 mg/cm^2, reducing the actual energy at the final surface by 0.15 to 0.20 MeV, depending on initial energy.

†The estimated uncertainty in the absolute concentrations is ≃ ± 50%, but the relative uncertainty is about ± 10%.

††Irradiated in channeling direction, but computations ignore this fact.

in stainless steel. In the sample of carburized stainless steel tubing shown in Fig. 21, the autoradiographs qualitatively indicate an increased carbon concentration to a depth of about 0.02 in. The black wedge at the lower right of the two autoradiographs is due to the activation of plotting plastic

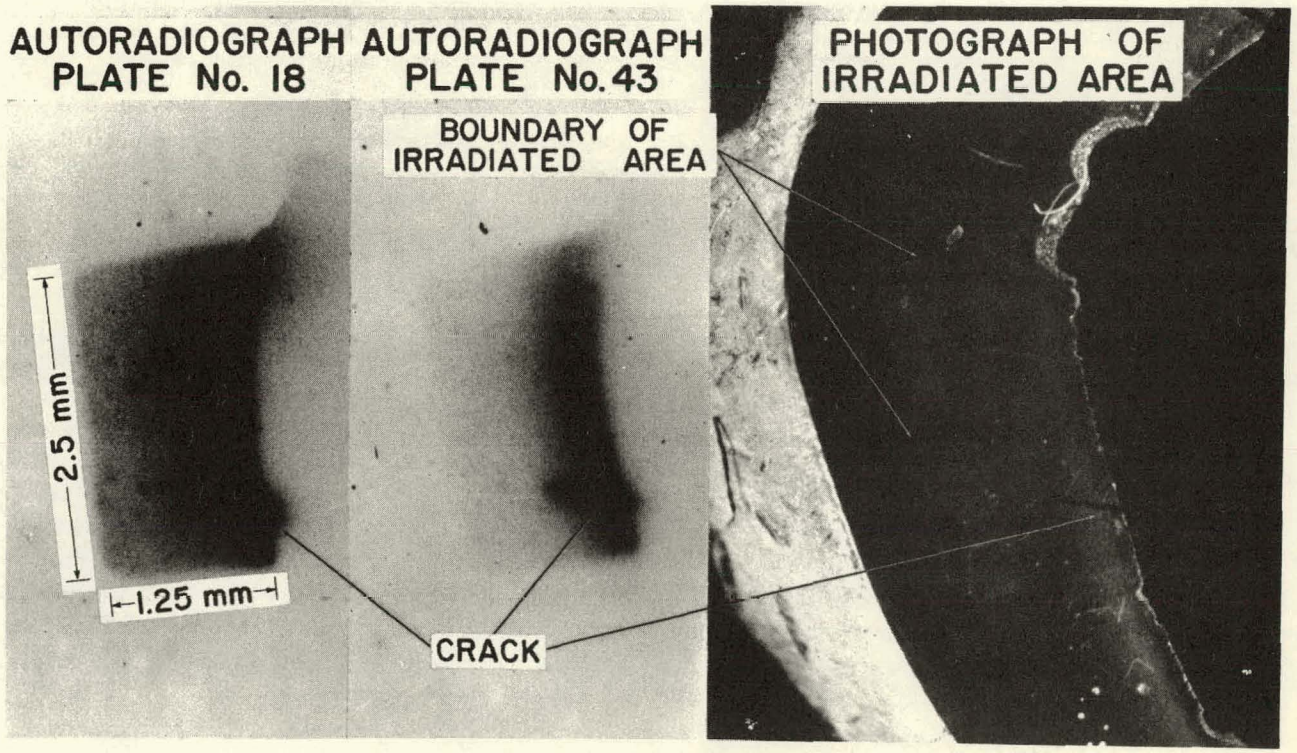

Fig. 21. Photograph and autoradiographs of ^{3}He-activated sample of carburized stainless steel.

in the crack in the sample (Fig. 21). Densitometric measurements of the autoradiographs interpreted with a calibration curve for the emulsion produce quantitative measurements of the carbon gradient. Figure 22 shows the carbon gradient (but not the absolute concentrations) for the sample in Fig. 21 as determined by three autoradiographs.

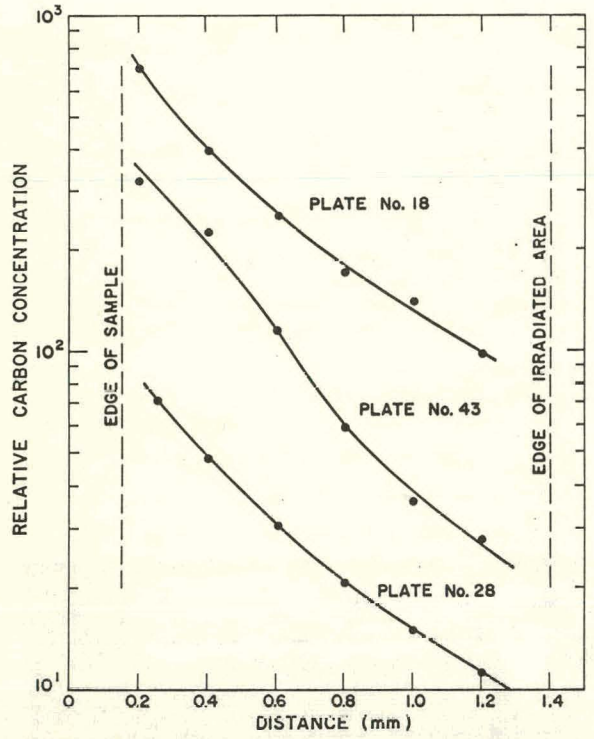

Fig. 22. Relative carbon concentrations in a carburized stainless steel sample determined by ^{3}He activation and autoradiography.

A program has been planned for further development and use of this technique for measuring the carbon gradient in stainless steel. Samples of Type 316 stainless steel tubing that have been carburized under different conditions will be analyzed to determine the carbon gradients. Samples of low- and normal-carbon Type 316 stainless steel will serve as standards for test and comparison.

Modifications for sample holders, both for performing the irradiations and obtaining the autoradiographs, have been designed and are being incorporated in the equipment. Tantalum foils and wires have been activated at the Omega West Reactor. From these activated samples, beta sources will be made with which to make preliminary studies of processing, resolution, and interpretation of the autoradiographs.

Preliminary study indicates that autoradiographic techniques similar to those used to determine the carbon gradient in stainless steel can be used to determine the distribution of copper in stainless steel. For copper in steel, photon activation by the reaction $^{65}Cu(\gamma n)^{64}Cu$ would be used. The half-life of ^{64}Cus is 12.9 h. Since this is much longer than the half-lives of beta-emitting products of (γ,n) reactions with iron, chromium, manganese, and carbon, autoradiographs of the copper distributions can be made after all the other beta activities have decayed to negligible levels.

XI. SYNTHESIS AND FABRICATION

(M. W. Shupe, C. A. Emery, H. G. Moore, R. W. Walker, R. L. Nance, A. E. Ogard)

A. General

Procedures have been developed for synthesizing and producing (U,Pu)C and (U,Pu)N pellets for compatibility testing. Unenriched (U,Pu)C pellets have been produced and stored. Recently the entire effort has been directed towards producing only fully enriched $U_{0.8}Pu_{0.2}C$ pellets for the EBR-II irradiation experiment which requires 52 pellets per pin. The present inventory for this experiment is 388 pellets. No effort has been allocated for preparation of nitride pellets for compatibility testing.

Carbide pellets are produced by the following method:

1. Multiple arc melting of U, Pu, and C on a 60 g scale using a graphite electrode.
2. Solution treatment of the ingot.
3. Crushing and grinding in a WC vibratory mill, followed by screening the resulting powder.
4. Reduction of excess carbon by reaction with flowing H_2.
5. Cold compaction followed by sintering in flowing Ar.

B. Current Results

Characteristics of the fourteen lots of pellets produced during this period are summarized in Table IV. At this time evaluation of the pellets is not fully complete. However, experience to date indicates that the MC_2 and M_2C_3 phases are eliminated from the pellet microstructure by the H_2 reduction

Table IV

Characteristics of Fully Enriched $U_xPu_yC_z$ Pellets

Lot No.	x	y	z	Quantity	Diam (in.)	% T.D.	Microstructure[1]
6-44-1	0.794	0.206	0.971	19	0.261	...	MC, I
6-44-2	0.800	0.200	0.974	17	0.260	...	MC, I
6-45-1	0.798	0.202	...	17	0.260	...	MC, I
6-47-1	0.798	0.202	...	17	0.264	90	MC
6-47-2	0.795	0.205	0.942	17	0.264	90	MC, I
6-53-1	0.795	0.205	0.984	17	0.267	85	MC
6-53-2	0.798	0.202	0.988	16	0.265	90	MC
6-53-3	0.801	0.199	...	16	0.262	...	MC, I
6-56-1	0.795	0.205	...	17	0.260	...	MC
6-56-2	0.796	0.204	...	18	0.267	...	...
6-56-3	0.799	0.201	...	17	0.266	...	...
6-74-1	0.797	0.203	...	58	≤ 0.263	90	MC
6-77-1	0.798	0.202	...	48	0.267	...	...
6-81-1	0.795	0.205	...	60	0.265	...	MC

(1) I indicates < 0.5 volume percent impurity phase containing U, Pu, Fe, Si, and/or Cu.

step. Of the 294 pellets from lots 6-44-1 through 6-77-1, all have been examined radiographically and 18 were found to have internal cracks. Each of the last three lots in Table IV were produced by blending powders from 3 smaller lots in order to improve diametral control.

Pellet sections have been examined by electron microprobe. The small amount of impurity phase (< 0.5 v/o) generally contains more plutonium than uranium, and always contains silicon, iron, and/or copper. Present efforts are directed towards reducing the concentrations of these metallic impurities. As shown in Table V, silicon content of the powder and pellet is influenced by relatively small amounts of silicon in the enriched uranium melting stock.

The particle size distributions of H_2 reduced (U,Pu)C powders are shown in Table VI. The mass median diameters of the five lots of reduced powders varied from 6.4 to 9.5 μ, while about 70 percent by wt. of the particles were in the 2 to 16.5 μ range. The particle size of powder lot 6-45-1 increased only slightly during the H_2 reduction treatment. Therefore size analysis on unreduced powders probably provides a good estimate of final powder particle size distribution. Pellet properties are being correlated with powder size distributions of these lots.

Table V

Spectrochemical Analysis of Enriched Uranium Melting Stock and (U,Pu)C Products

	Element Conc. ($g/10^6$ g Pu)			
	Lot 9-142-1		Lot 5801	
Element	Melting Stock	MC Pellets	Melting Stock	MC Powder[1]
Li	< 0.5	< 1	< 0.2	< 1
Be	< 0.1	< 1	< 0.1	< 1
B	< 0.2	< 1	< 0.4	< 1
Na	2	< 2	3	2
Mg	2	< 5	5	< 5
Al	15	< 10	15	10
Si	150	200	75	60
P	< 50	< 50	< 50	< 50
Ca	< 2	< 5	5	< 5
V	30	< 5	10	< 5
Cr	3	< 10	10	< 10
Mn	3	5	10	< 2
Fe	70	60	90	95
Co	< 5	< 5	< 5	< 5
Ni	300	40	10	< 10
Cu	5	100	3	50
Mo	< 25	< 10	< 25	< 10
Cd	< 1	< 10	< 1	< 10
Sn	< 1	< 2	< 1	< 2
Pb	< 1	< 2	< 2	< 2
W	< 100	< 10	< 100	10

(1) Pellet analysis not yet completed.

Table VI

Particle Size Distributions of Hydrogen Treated (U,Pu)C Powders

Lot No.	Maximum Size Mesh (μ)	Size (μ) Greater than 20 w/o	40 w/o	50 w/o	70 w/o	90 w/o
6-44-1	325 (44)	16.5	9	6.7	3.6	1.9
6-44-1	325 (44)	16.8	9	6.4	3.5	1.8
6-45-1[1]	325 (44)	16.0	8.3	5.9	3.1	1.5
6-45-1	325 (44)	16.5	9	6.6	3.7	1.9
6-53-2	200 (74)	28[2]	13	9.4	4.6	2.3
6-56-3	230 (64)	24[2]	13	9.5	4.9	2.2

(1) Powder prior to hydrogen treatment.
(2) By graphical extrapolation.

REFERENCES

1. F. B. Litton, "The Behavior of Carbide Fuels: A Literature Survey," Report LA-3799, Los Alamos Scientific Laboratory.
2. B. J. Thamer, "The Use of (U,Pu)N Fuel with a Sodium Bond: A Summary of Existing Data," Report LA-3646, Los Alamos Scientific Laboratory, March 27, 1967.
3. D. B. Hall et al., "Compatibility of Sodium Bonded (U,Pu)C and (U,Pu)N Fuels with Cladding Materials," Project 808, "Quarterly Status Report on the Advanced Plutonium Fuels Program, April 1 - June 30, 1967," Report LA-3745-MS, Los Alamos Scientific Laboratory August 30, 1967.
4. H. E. Chamberlain and E. L. Paige, "A Metallographic Technique for Distinguishing Between Metal and Sesquicarbide Phases in the U-C and (U,Pu)C Systems," U.K.A.E.A., Harwell, Report HL 63/2866, United Kingdom Atomic Energy Authority.
5. C. C. Land, Los Alamos Scientific Laboratory, private communication.

PROJECT 811

REACTOR PHYSICS

Person in Charge: D. B. Hall
Principal Investigator: G. H. Best

I. INTRODUCTION

Basic to the evaluation of various fast breeder concepts and proposals are the analytical techniques and physical data used in the analyses. Valid comparisons between different concepts and proposals depend on minimization of differences in results due to the methods of analysis. To this end, the Los Alamos Scientific Laboratory is cooperating with other AEC laboratories and contractors in the development of evaluated cross-section data and associated processing codes. This work is correlated through the Cross Section Evaluation Working Group (CSEWG), which is made up of representatives of the various organizations. In addition, the Laboratory is working on the development and maintenance of digital computer programs pertinent to the nuclear analysis of fast breeder concepts. Finally, the Laboratory is evaluating the performance characteristics of various fast breeder reactor concepts.

II. CROSS-SECTION PROCUREMENT, EVALUATION, AND TESTING (M. E. Battat, D. J. Dudziak, R. J. LaBauve)

A. General

Accurate predictions of reactor design parameters, such as critical mass, sodium worth, and spectral response, require the development and maintenance of up-to-date basic microscopic nuclear data files. To meet this need, a national cooperative program is in progress to prepare an evaluated nuclear data file (ENDF/B).

B. Data Testing

Tapes 114, 115, 116, and 999 have been received from Brookhaven National Laboratory containing ENDF/B data in a "Category I" status, that is, data approved by the Data Testing Subcommittee for general distribution. The contents and current disposition of the BNL tapes are summarized in Table I. As received from BNL, the data tapes are in "Mode 3" -- BCD card image form. The data must be converted to a binary form -- "Mode 2" -- by the code DAMMET[1] before it can be used as input to ETOE. ETOE is then used to write a data tape in a format suitable for MC^2. Multigroup cross sections from MC^2 are converted to the DTF format by a locally devised code, XSCCN.

A corrected version of MC^2 is now running on the CDC 6600. Also, corrections for ETOE have been incorporated in our version of this code, and a data tape was made for MC^2 with the latest ENDF/B (Category I) data. From this data tape and from the original Argonne National Laboratory data tape, 16-group cross sections were derived for the Jezebel critical assembly with the new version of MC^2. These cross sections were then used in the DTF code[2] to calculate the critical radius for Jezebel. Results are compared with earlier calculations in Table II.

It should be noted that the energy group structure used for the MC^2 calculations is very nearly that of the Hansen-Roach set, with the lowest energy cut at 0.414 eV. The experimental critical radius for Jezebel is 6.284 cm.

With the multigroup constants generated by MC^2, problems are being run to obtain perturbation cross sections for various materials in Jezebel. Work is also underway to generate multigroup constants for ZPR-3, Assembly 48.

TABLE I

CATEGORY I ENDF/B MATERIALS
As of November 20, 1967

Material	Material No.	BNL Tape No.	LASL Tape No. Mode 3 Tape	LASL Tape No. Mode 2 Tape	MC^2 Lib. Tape 9
H	1001	115	HM012	GG048	
D	1003	115	HM012	↓	
^{6}Li	1005	114	EF027		
Be	1007	116	GM074	-----	
^{10}B	1009	114	EF027	GG048	
^{12}C	1010	114	↓	↓	GM026
^{14}N	1012	114			
^{16}O	1013	115	HM012		
Mg	1014	114	EF027		
Ti	1016	114	↓		
V	1017	114			
Cr	1018	115	HM012		GM026
Mn	1019	114	EF027		
Fe	1020	115	HM012		GM026
Ni	1021	115	HM012		GM026
Nb	1024	116	GM074	-----	
Mo	1025	114	EF027	GG048	
^{135}Xe	1026	115	HM012	↓	
^{149}Sm	1027	115	HM012		
^{151}Eu	1028	116	GM074	-----	
^{153}Eu	1029	116	GM074	-----	
Gd	1030	114	EF027	GG048	
^{164}Dy	1031	116	GM074	-----	
^{175}Lu	1032	116	↓	-----	
^{176}Lu	1033	116		-----	
Hf	1034	999	GM074	-----	
^{181}Ta	1035	114	EF027	GG048	
^{197}Au	1037	116	GM074	-----	
^{233}U	1041	999	GM074	-----	
$^{233}U^{a}$	1042	114	EF027	GG048	
^{234}U	1043	115	GM012	GG048	
^{235}U	1044	116	GM074	-----	
$^{235}U^{a}$	1045	114	EF027	GG048	
^{236}U	1046	115	HM012	↓	
^{238}U	1047	115	HM012		GM026
^{237}Np	1048	116	GM074	-----	
^{238}Pu	1050	116	GM074	-----	
^{239}Pu	1051	115	HM012	GG048	GM026
$^{239}Pu^{a}$	1052	114	EF027	↓	
^{240}Pu	1053	114	EF027		GM026
^{241}Pu	1054	114	HM012		GM026
^{242}Pu	1055	116	GM074	-----	
^{241}Am	1056	115	HM012	GG048	
^{243}Am	1057	115	HM012	GG048	
^{244}Cm	1058	116	GM074	-----	
^{23}Na	1059	114	EF027	GG048	GM026
^{182}W	1060	↓	↓	↓	
^{183}W	1061				
^{184}W	1062				
^{186}W	1063				
$^{233}U^{b}$	1066				
$^{233}U^{c}$	1067				
$^{235}U^{b}$	1068				
$^{235}U^{c}$	1069				
$^{239}Pu^{b}$	1070				
$^{239}Pu^{c}$	1071				
^{176}Hf	1072	999	GM074	-----	
^{177}Hf	1073	↓	↓	-----	
^{178}Hf	1074			-----	
^{179}Hf	1075			-----	
^{180}Hf	1076			-----	
^{184}Hf	1082			-----	

[a] RSFP = Rapidly saturating fission products
[b] SSFP = Slowly " " "
[c] NSFP = Nonsaturating " "

TABLE II

JEZEBEL CRITICAL RADIUS CALCULATIONS

Cross-Section Set	No. of Groups	Radius (cm)
Hansen-Roach[3]	16	6.281
Russian[4]	26	6.135
Derived from ANL Library (MC^2)	14	6.196
Derived from ENDF/B Library (MC^2)	14	6.209

With the ETOE code, an MC^2 library tape has been prepared for ^{6}Li, ^{7}Li, Be, ^{10}B, ^{12}C, Cr, Fe, Ni, Mo, ^{235}U, ^{236}U, ^{238}U, ^{239}Pu, ^{240}Pu, ^{241}Pu, ^{242}Pu, and ^{23}Na. The inelastic scatter transfer matrices for C, Cr, and Ni are incomplete on this tape. For C, the inelastic secondary-energy distributions were not given in the ENDF/B tape; for Cr and Ni, the distributions given were not accepted by MC^2 because of format incompatibilities. An attempt is being made to remedy these deficiencies.

C. Shielding

A code to translate cross-section data from the UK format to the ENDF/B format is now being debugged. The code, LATE (Los Alamos Translation to ENDF/B), reads the restricted case of the UK format which was used by Drake et al.[5] for their evaluation of sodium, magnesium, chlorine, potassium, and calcium. It will be used to translate these data and an evaluation of silicon which Drake is now preparing.

III. REACTOR ANALYSIS METHODS AND CONCEPT EVALUATIONS

A. Space-Time Reactor Kinetics Codes

1. Synthesis Method (J. C. Vigil)

The space-time synthesis method which results in the multimode equations has been programmed for the CDC-6600 computer. The code consists of two separate programs, PARAS and ANCONM. PARAS computes the parameters which appear in the multimode equations by using fluxes and currents for various trial functions computed with the DTF code. These parameters are then input to the ANCONM code, which solves the multimode equations by continuous analytic continuation and performs the space-time synthesis by combining the trial functions with the solutions to the multimode equations.

The code is presently limited to one space dimension in any geometry, step reactivity perturbations (in microscopic cross sections and/or atom

densities), with no reactivity feedback. Any number of delayed neutron groups are allowed. PARAS also computes the parameters required by the conventional point kinetics equations.

One test problem has been run, with encouraging results. Comparisons with point kinetics and the WIGL2 code[6] are planned.

2. Multienergy-Group Method (G. C. Hopkins)

ANCONMG, a multienergy-group kinetics code, has been compiled and is currently undergoing minor revisions to reduce the computing times required for typical transient analyses.

Although a detailed comparison has not yet been made for a problem run with both ANCON[7] and ANCONMG, preliminary results indicate that computing times for a transient run with ANCONMG are about five times as long as those for ANCON. This is principally due to two facts:

1. Whereas ANCON solves the kinetic equations for one average energy group, ANCONMG solves these equations explicitly for each of the energy groups specified, and
2. Because the lifetimes in the fast groups are much shorter than the average lifetime, the time steps are also much shorter, resulting in increased computing times.

An initial study has shown that a six-energy-group analysis is not feasible with ANCONMG. Because very short lifetimes are associated with some of the fast groups, the computing time requirements are prohibitive for normal transient analysis. Therefore, a two-energy-group set of parameters is being prepared for study.

B. Preparation and Maintenance of Code Packages (B. M. Carmichael, R. L. Cubitt)

A code (MDTF) using some of the standard DTF subroutines[2] has been developed to compute homogenized cell cross sections. This code has the advantage that for input it uses the cell DTF input deck intact and requires only the addition of the cell fluxes. This code will be enlarged to accommodate perturbation calculations and to obtain reactor performance figures, such as reaction rates for breeding ratio and specific power.

C. Blanket Design Studies (M. E. Battat, R. L. Cubitt)

With U-Pu-Th alloy as core fuel, preliminary calculations have been made to determine the effects of varying Pu concentrations in the blanket. Both metal (U-Pu-Zr) and oxide (UO_2) blanket materials were studied.

Calculations were made with the DTF-IV neutron transport code[2] in the S_4 approximation and the 16-group Hansen-Roach cross-section set. The geometry assumed was an infinite cylinder with either a 10- or 20-cm-radius core surrounded by a 30-cm-thick blanket. A reflective outer-boundary condition was specified, i.e., no radial leakage. For selected blanket ^{239}Pu concentrations in the 2 to 5% (of total heavy atoms) range, problems were run in which criticality was achieved by adjusting the core ^{239}Pu concentration. This adjustment was made subject to the constraint that the sum of the heavy atoms -- plutonium, uranium, thorium, and fission products -- remained constant. The fact that, in some cases, the resulting relative concentrations of uranium, plutonium, and thorium might not constitute a practical fuel was not considered.

With regard to fraction of fissions which occur in ^{238}U, blanket multiplication, and blanket power fraction, metal blankets seem more promising than oxide blankets. However, the oxide blanket does give more favorable sodium voiding effects.

Similar calculations were made for a core consisting of coated particles in a uranium matrix surrounded by a metal uranium blanket. Insofar as blanket performance and breeding ratios are concerned, the coated-particle fuel is more attractive than either the metal- or oxide-blanket systems. However, the core sodium void coefficient for the coated-particle system is more positive than that for either the metal- or oxide-blanket configurations with U-Pu-Th as core fuel.

REFERENCES

1. Explanations of ENDF/B codes appear in the last quarterly report on this program, "Quarterly Status Report on the Advanced Plutonium Fuels Program, July 1 - September 30, 1967," LA-3820-MS, Los Alamos Scientific Laboratory, 1967.

2. K. D. Lathrop, "DTF-IV, A FORTRAN-IV Program for Solving the Multigroup Transport Equation with Anisotropic Scattering," LA-3373, Los Alamos Scientific Laboratory, 1965.

3. "Los Alamos Group-Averaged Cross Sections," L. D. Connolly, ed., LAMS-2941, Los Alamos Scientific Laboratory, 1963.

4. "Group Constants for Nuclear Reactor Calculations," I. I. Bondarenko, ed., Consultants Bureau Translation, 1964.

PROJECT 822

EXAMINATION OF FAST REACTOR FUELS

Person in Charge: R. D. Baker
Principal Investigators: J. W. Schulte
J. A. Leary
C. F. Metz

I. INTRODUCTION

This project is directed toward the examination and comparison of the effects of neutron irradiation on LMFBR Program fuel materials. Irradiated materials will be examined as requested by the Fuels and Materials Branch of DRD & T.

II. FUEL CAPSULE HANDLING CAPABILITY

(F. J. Fitzgibbon, P. J. Peterson, A. E. Tafoya, J. R. Trujillo)

Design of the cask for shipping irradiated capsules (in a vertical position) from EBR-II to LASL is currently being analyzed to determine if the shielding is adequate for 19 capsules irradiated to 100,000 MWD/T and with only 15 days cooling. Both depleted U and Pb are still being considered for the shielding material. A Special Task Force at LASL will review the final design for compliance with the requirements as set forth in Chapter 0529 of the AEC Manual. It is anticipated that the drawings will be submitted to the AEC for certification about March 1, 1968.

Additional tests have been conducted for a careful examination of potential problem areas in unloading, transferring and general remote handling of irradiated capsules. As a result of these tests, modifications have been made to some of the handling fixtures, and additional illumination was installed to provide better viewing of the unloading operations.

III. INERT ATMOSPHERE BOXES

(M. D. Keehn, R. F. Velkinburg)

Five alpha boxes which were ordered for this program have been received and are in the process of being equipped with viewing ports, light wells, transfer systems, service connections, etc. When all basic equipment has been assembled, the boxes will be He leak tested to assure that proper seals have been obtained. At this point the equipment is installed and cold runs will be started.

The recirculating Ar purification system, having a capability of processing 20 SCFM with an impurity level of < 1 ppm H_2O or O_2, was received in early December. All service connections and instrumentation have been installed on an alpha box. The pressure controls and backup controls on the purifier unit have been checked and adjusted as required.

Preliminary tests indicate that the Moisture Monitor and Oxygen Analyzer are performing satisfactorily. The operating efficiency of the system will be determined in the next test which involves purging the alpha box with Ar until the O_2 concentration has decreased to ~ 1000 ppm, at which time the recirculating purification unit is connected to the system. Several tests will be conducted to ascertain: the capacity of the system; the atmosphere purity which can be obtained; the effect of various operations, such as transfers into the box on atmosphere purity; and such other experiments as may be required in proof tests.

IV. IN-CELL EQUIPMENT

(G. R. Brewer, E. L. Ekberg, M. W. McCloskey, G. H. Mottaz, F. H. Newbury, P. J. Peterson, T. Romanik)

Inert Gas System for Transfer Containers

The purpose of this system is to limit the quantity of O_2 introduced into the high purity alpha box during transfer operations. Additional tests in which the containers are evacuated to $<200\ \mu$ and then pressurized to 1 psi of Ar before attachment to the alpha box have been successfully completed.

Removal of Cladding From Fuel

Satisfactory tests have been run with the stripping fixture on unirradiated material. The success of this device on removing irradiated clad will not be known until suitable test material is received.

If the fuel has swelled or reacted with the clad sufficiently to preclude use of the stripping fixture, other methods of clad removal will be tried, such as slitting or sectioning. A saw for this purpose is in the fabrication stage.

Dimensioning Equipment

Equipment for taking dimensions of both capsules and pellets have been fabricated and tested. Sensitivities of ~ 0.0002 in. are possible on diametral measurements of the capsule, and on diameter and length of the pellets. The pellet dimensioner will also indicate bulged and dished ends as well as perpendicularity of the pellets.

Fission Gas Sampling

The system for puncturing the clad and taking gas samples from the capsules in an inert atmosphere box has not yet been evaluated.

Gamma Scanning

Design of the equipment for carrying out this operation in the hot cells is nearly complete. Fabrication is expected to be completed by April 1968.

X-ray Radiography

The cask and transfer equipment for this operation are available and appear to be satisfactory.

Na Distillation

The distillation unit is currently being fabricated. A special holder for the pellets was constructed which will serve the following functions: permit viewing of top, bottom and sides; store the pellets in holes for identification; and serve as the holder during distillation of the Na.

Density Measurements

Preliminary experiments are under way to determine the densities of thermally hot pellets by using Hg as the immersion medium. Both W and Ta are being considered as construction material for the basket.

V. DIFFERENTIAL THERMAL ANALYSIS

(D. B. Court)

Fabrication of the oscillator and control unit for the furnace was completed. Tests run to date indicate satisfactory performance. Construction of the furnace has been completed; the furnace and generator are being temporarily installed in a "cold" area for initial testing. Design work on installation of the equipment in the hot cell has been finished, and detail drawings of component items have been released for fabrication.

VI. HEAT CONTENT MEASUREMENT

(C. E. Frantz)

After a careful evaluation of methods for obtaining heat content measurements, it was concluded that a recirculating water constant temperature bath (similar to that previously described)[1] with an isothermal calorimeter located in the hot cell was most promising for remote application. Design of the bath system is under way; whereas the design of the W mesh furnace will be started when results from a similar unit (currently being fabricated) are known. A sample drop mechanism was mocked-up and successfully tested at room temperature. Design of the fixture for welding the capsule remotely is complete and fabrication has started. Controls and services for the welding fixture are in the design phase.

Sufficient data have been collected to determine that temperature measurements by optical pyrometry can be made through a Pb glass window, 32 in. thick. Experimental errors by this method are less than or equal to those encountered with a periscope arrangement. Temperature errors appear to be in the range of 0.25-1%. One of the chief difficulties in this method is selecting a section of the window without flaws, which cause some optical distortion and introduce errors in the temperature measurements. However, the flaws can be easily avoided by selecting an area of the window which is free of optical distortion.

VII. HOT CELL METALLOGRAPHY

(K. A. Johnson, M. W. McCloskey)

The hot cell metallograph and all the mounting and polishing equipment are now fully operational. This equipment has all been tested with simulated fuel materials. Metallographic capabilities have been improved to the point where 12 samples per day can be mounted and polished. The limit on specimen examination now will be the number and types of tests or operations that are required on the polished specimens, i.e., hardness, microphotography, autoradiography, etc.

A vacuum potting chamber has also been installed and tested. This new capability to pot specimens under vacuum will greatly help in mounting cracked, porous, or thin specimens.

A holder for checking the quality of polish of specimens while still in the specimen mount holder has been installed and tested. This attachment allows the use of the hardness tester microscope for interim examination before removing the 6 finished specimens from the mount holder.

VIII. ANALYTICAL CHEMISTRY

(O. R. Simi, J. H. Dahlby, C. S. MacDougall, T. K. Marshall)

Spectrochemical Analysis of Irradiated U-Pu Fuels

A carrier-distillation technique has been tested in the analytical hot cell using unirradiated UC_2 as a stand-in material. The sample was crushed, ignited, mixed with 6% Ga_2O_3 as a carrier, and excited with a d.-c. arc in a controlled atmosphere of O_2-30% Ar. The method was found to be applicable to the following impurity elements (lower limits of detection are indicated in ppm): Be and B, 0.3; Sn and Mg, 2; Al, 5; P, Sr, Ca and V, 30; Cr, 3; Fe, Pb, Bi, Ni, Mo and Si, 6; Mn and Cu, 0.6; Cd and Zn, 20.

All apparatus design for remote control operations in the hot cell worked satisfactorily.

Testing of Microliter Pipets

Hot cell tests were made of commercial, self-sealing, disposable micropipets, which were made of short lengths of precision-bore capillary glass tubing. Repeated measurements were made by weighing, filling and reweighing which indicated an overall reproducibility (1σ) of <1% for aliquoting volumes 1 and 100 $\mu\ell$. This precision is considered good and use of this type of pipet for aliquoting hot solutions is planned.

The Determination of Oxygen in Irradiated Fuels

A fused silica furnace designed for the application of an inert-gas fusion technique to determine oxygen in irradiated fuels was tested under simulated hot cell conditions. Equipment designed for hot cell operations such as pulverizing fuel pellets, blending powders and pressing fuel sample and powdered graphite into pellets was also tested. All equipment behaved satisfactorily and it is planned to use it in the analysis of irradiated materials.

The Determination of Free (Uncombined) Carbon in Carbide Fuels

Equipment is being designed for hot cell operation in the analysis of irradiated materials. The fused silica furnace was inadequate for the intended operation and a new design is now being fabricated.

IX. EXAMINATION OF EBR-II DRIVER FUEL

(K. A. Johnson, J. W. Schulte, G. R. Waterbury)

At the request of the Division of Reactor Development and Technology, LASL will do an extensive study on 6 irradiated EBR-II Driver Fuel Rods.

Three unirradiated rods were received on December 21 for the purposes of checking in-cell equipment, dissolution tests, radiography tests, etc. Additional rods, 2 unirradiated and 6 irradiated, are expected to arrive at LASL by January 5, 1968

X. PROCUREMENT OF IRRADIATED $(U,Pu)O_2$ FUELS

(J. W. Schulte)

Approximately 40 g of mixed oxide fuel irradiated to 100,000 MWD/T will be supplied by G.E. Vallecitos for the purpose of checking out remote equipment and techniques. It is expected that this material will arrive at LASL about January 10, 1968.

XI. EXAMINATION OF UNIRRADIATED FUEL

Plastic Deformation

(M. Tokar, A. L. Gonzales)

Installation of the apparatus in the glovebox enclosure

is essentially complete. The design of this equipment is based on that now in use on UC-graphite composites.[2] It is designed to operate under vacuum or under an inert atmosphere at a maximum temperature of 2500°C, and a maximum pressure of 8000 psi. The specimen is heated by an induction coil which is powered by a 15 KVA Motor-generator set. This provides the capability for changing specimen temperature rapidly, which is desirable in determining activation energies for creep by the Dorn method.[3]

Specimens of UC have been sintered to form 1/2-in. diam x 1/2-in. long cylinders for preliminary test of the equipment before committing it to use with plutonium materials.

Thermal Conductivity
(K. W. R. Johnson)

The 3M, Model TC-200 comparative type thermal conductivity apparatus has been modified for use on plutonium materials, and to improve its capabilities.

A new thermocouple system has been fabricated and calibrated with N.B.S. melting point standards.

The thermal conductivity of a 1-in. diam x 1-in. long Inconel 702 standard specimen was measured between 101° and 1212°C. In the range 101-750°C, the measured thermal conductivities were within ±2% of the recommended values.[4] At 1212°C, the conductivity was 12% low. Present efforts are being directed towards evaluating the instrument for use on 1/2-in. diam x 1/2-in. long specimens in the high temperature ranges.

Hot Hardness
(K. A. Johnson, A. L. Gonzales)

Fabrication of the hot hardness instrument for plutonium ceramic fuel materials is complete and the unit has been assembled in the cathodic-etching glovebox. Installation of services should be completed in March, at which time the instrument will be committed for use on plutonium materials.

Vacuum Cathodic Etching
(K. A. Johnson, A. L. Gonzales)

Fabrication of the instrument is complete, and it is installed in the plutonium glovebox enclosure. Installation of electrical and vacuum service to the enclosure by the crafts remains to be done.

XII. REFERENCES

1. "Quarterly Status Report on the Advanced Plutonium Fuels Program, July 1 - September 30, 1967," LASL Report No. LA-3820-MS, p. 21 (1967).
2. K. V. Davidson, R. E. Riley, J. M. Taub, "Carbide-Graphite Composites," Report LA-3569-MS, Los Alamos Scientific Laboratory (1966).
3. John E. Dorn, "The Spectrum of Activation Energies for Creep," Creep and Recovery, Amer. Soc. for Metals (1957).
4. D. R. Flynn, National Bureau of Standards Report 7836, March 1963.

XIII. PUBLICATIONS

J. A. Leary and K. W. R. Johnson, "Thermal Conductivity of Uranium-Plutonium Carbide Fuels," Nuclear Metallurgy Symposium on Plutonium Fuels Technology, A.I.M.E., Phoenix, Oct. 4-6, 1967, LASL Report No. LA-DC-9059.

OTHER ADVANCED SYSTEMS - RESEARCH AND DEVELOPMENT

Person in Charge D. B. Hall
Principal Investigators: R. H. Perkins
E. O. Swickard

I. AQUEOUS NEUTRON SOURCE
(B. J. Thamer)

A. General

One version of the Liquid Excursion Pulsed Reactor (LEPR)[1] may be envisioned as having 0.864 molar enriched uranyl sulfate. The desired concentration would be decided partly by the size and shape of the neutron pulse to be attained. The 0.864 molar solution might furnish about 2 megajoules per liter per pulse. There would be the hazard of precipitating uranium peroxide because part of the fuel solution could remain below 150°C and the radiolytic hydrogen peroxide would not decompose instantly at those temperatures. It may be estimated from available data that the concentration of generated peroxide is approximately 1×10^{-7} x (number of joules per liter) at any point in the solution. Ignoring the effect of sulfate complexing, the precipitation of uranium peroxide can be represented by the equation

$$UO_2^{+2} + H_2O_2 = UO_4\downarrow + 2\ H^+$$

for which the equilibrium constant at room temperature is about 300. Excess sulfuric acid may be used to repress the reaction in tests to render hydrogen peroxide soluble in 0.864 molar uranyl sulfate.

When the necessary concentration of sulfuric acid has been ascertained then the thermal stability of the resulting solution should be examined. This may be done out-of-pile by exposing a small sample to a 6-joule 15-nanosecond pulse from a ruby laser. The laser beam is made to converge on the quartz-encapsulated sample by means of a lens. The vaporized and condensed solution then is centrifuged to one end of the capillary for comparison with its original state.

B. Current Results

Preparations are being made to determine the necessary levels of sulfuric acid to prevent peroxide precipitation at various temperatures.

The laser test of thermal stability has been applied to 3.12 molar uranyl sulfate containing no excess sulfuric acid. There was no obvious decomposition of the solution. In the future the composition of any solution under test will be determined by scanning the capillary spectrophotometrically before and after the laser pulse.

In addition to the above, neutron-source measurements with enriched uranyl sulfate solutions are planned. Tests will be carried out on solutions both with and without depletion of oxygen-17 and -18.

II. HIGH TEMPERATURE NEUTRON DETECTOR TEST
(E. O. Swickard)

Two high temperature neutron detectors were purchased from each of three manufacturers for evaluation. The detectors have ^{235}U coated electrodes with integral, mineral-insulated cables. Specifications required that both the detector and cable operate at 600°C. Test objective is the determination of the effect of temperature on the following: (1) pulse height distribution; (2) neutron counting sensitivity; (3) detector and cable resistance; (4) detector and cable capacitance; and (5) detector and cable noise.

Detectors with their integral cables are installed in four 17-ft high furnaces that contain a helium atmosphere at a few psig. Electrical heaters

on the outside of the furnace tube are wired so that those in the detector region and those in the cable region are independently controllable.

The integral cable is connected to a preamp which drives an amplifier whose output drives a scaler and a 400-channel pulse height analyzer. Counts are taken with and without a neutron source just outside the furnace insulation. Temperature is raised at 100°C increments. The testing schedule is shown in the following table.

Temp. °C		2 minute counts O.V.-	O.V.	O.V.+	Measure R and C
25-50	N	X	X	X	X
	n	X	X	X	
100	N	X	X	X	X
	n	X	X	X	
25-50	N		X		X
	N		X		
200	N	X	X	X	X
	n	X	X	X	
'		'	'	'	'
'		'	'	'	'
'		'	'	'	'
600	N	X	X	X	X
	n	X	X	X	
25-50	N	X	X	X	X
	n	X	X	X	
600 (500 hr)	N	X	X	X	X
	n	X	X	X	

O.V. = Mfr recommended operating voltage

R = Resistance of detector and lead

C = Capacitance of detector and lead

N = No source counting

n = Neutron source counting.

In addition to the testing schedule above, one detector from each manufacturer will be tested at 25 and 50°C above the specification temperature of 600°C, provided the detector is in operable condition after 600°C testing.

Status of testing is shown below:

Detector Ident.	25-600°C	600°C (500 hr)	625 and 650°C
W-1	completed	completed	not scheduled
W-2	completed	completed	in progress
RS-1	completed	completed	not scheduled
RS-2	completed	completed	in progress
GE-1	completed	in progress	
GE-2	completed	in progress	

All six detectors have operated satisfactorily at 600°C. One of the six became inoperable after a week at 600°C. Although all tests have not been completed, it is concluded that all three manufacturers are capable of supplying neutron detectors of fission counter type that can operate with detector and cable temperatures up to 600°C and possibly to 650°C.

III. EQUATION OF STATE OF REACTOR FUELS
(E. O. Swickard)

Fast reactor accident analysis requires equation of state for fuel materials at high temperatures. Currently this information is obtained by extrapolation of available low temperature data using an assumed model. Results of such an extrapolation are dependent on the model used and there is little to indicate which model gives correct information.

Shock transient time measurements have been used to calculate material equation of state for high pressures and low temperatures. By reducing material density, the same technique may be able to give equation of state of reactor fuel for temperatures and pressures of interest in reactor accident analysis.

A program is underway to investigate the feasibility of: (1) Fabricating reactor fuel samples with a range of densities down to about one-fourth normal density. (2) Making shock transient time measurements on a series of different density material to find if the method will yield equation of state in the range of interest.

The next material to be measured is UC. Preliminary work on preparation of low density UC has been started. Samples having densities below about 60% of crystalline appear to be difficult to make.

REFERENCES

1. L. D. P. King in Program Status Report, Weapons Research and Development, Part I, July 1 - Sept. 30, 1967, Report DIR-2103, Los Alamos Scientific Laboratory.

SPECIAL DISTRIBUTION

Atomic Energy Commission, Washington

Division of Research

D. K. Stevens

Division of Naval Reactors

R. Hawthorne

Division of Reactor Development and Technology

Lewis J. Colby
G. W. Cunningham
Donald E. Erb
Nicholas Grossman
Kenneth E. Horton
R. E. Pahler
J. M. Simmons (2)
Edward E. Sinclair
A. Van Echo
G. W. Wensch
M. J. Whitman
I. F. Zartman (2)

Division of Space Nuclear Systems

G. K. Dicker
F. C. Schwenk

Idaho Operations Office

DeWitt Moss

Ames Laboratory, ISU

O. N. Carlson
W. L. Larsen
M. Smutz

Argonne National Laboratory

Alfred Amorosi
Frank G. Foote
Sherman Greenberg
J. R. Humphreys
J. H. Kittel
R. E. Macherey
M. V. Nevitt

Idaho Falls, Idaho

D. W. Cissel

Atomics International

R. W. Dickinson, Director
Liquid Metals Information Center

C. E. Wobor

Babcock & Wilcox Co.

C. Baroch
J. H. MacMillan

Battelle Memorial Institute

Donald L. Keller
Stan J. Paprocki

Brookhaven National Laboratory

D. H. Gurinsky
C. Klamut

Combustion Engineering, Inc.

S. Christopher

Donald W. Douglas Laboratories

R. L. Andelin

General Electric Co., Cincinnati, Ohio

V. P. Calkins

General Electric Co., Sunnyvale, Calif.

R. E. Skavdahl

General Electric Co., KAPL

W. M. Cashin

Gulf General Atomic Inc.

Donald V. Ragone

Idaho Nuclear

W. C. Francis

IIT Research Institute

R. Van Tyne

Lawrence Radiation Laboratory

Leo Brewer
J. S. Kane
A. J. Rothamn

Mound Laboratory

R. G. Grove

NASA, Lewis Research Center

J. J. Lambardo

Naval Research Laboratory

L. E. Steele

Oak Ridge National Laboratory

G. M. Adamson
J. E. Cunningham
J. H. Frye, Jr.
C. J. McHargue
P. Patriarca
O. Sisman
M. S. Wechsler
J. R. Weir

Pacific Northwest Laboratory

F. W. Albaugh
E. A. Evans

Pacific Northwest Laboratory

FFTF Project

E. R. Astley
B. M. Johnson
D. W. Shannon (2)

Bureau of Mines, Albany, Oregon

H. Kato

United Nuclear Corp.

A. Strasser

Westinghouse Atomic Power Division

R. J. Allio

Westinghouse, Bettis Atomic Power Laboratory

E. J. Kreigh